Polymorphism of spironolactone: An unprecedented case of monotropy turning to enantiotropy with a huge difference in the melting temperatures

Ivo B. Rietveld, Maria Barrio, Pol Lloveras, René Céolin, Josep-Lluis Tamarit

POLYMORPHISM OF SPIRONOLACTONE: AN UNPRECEDENTED CASE OF MONOTROPY TURNING TO ENANTIOTROPY WITH A HUGE DIFFERENCE IN THE MELTING TEMPERATURES

Ivo B. Rietveld [a,b,*], Maria Barrio [c], Pol Lloveras [c], René Céolin [d], Josep-Lluis Tamarit [c]

[a] Normandie Université, Laboratoire SMS-EA3233, Université de Rouen, F76821, Mont Saint Aignan, France

[b] Faculté de Pharmacie, Université Paris Descartes, USPC, 4 avenue de l'observatoire, 75006 Paris, France

[c] Grup de Caracterització de Materials, Departament de Física and Barcelona Research Center in Multiscale Science and Engineering, Universitat Politènica de Catalunya, EEBE, Campus Diagonal-Besòs, Av. Eduard Maristany 10-14, 08019 Barcelona, Catalonia, Spain

[d] LETIAM, EA7357, IUT Orsay, Université Paris Sud, rue Noetzlin, 91405 Orsay, France

* Corresponding author: ivo.rietveld@parisdescartes.fr, +33 1 53739675

ABSTRACT

Spironolactone form I melts at about 70 degrees lower than form II, which is very unusual for two co-existing polymorphs. The phase relationships involving this unprecedented case of dimorphism have been investigated by constructing a topological pressure-temperature phase diagram. The transition from polymorph I to polymorph II is unambiguously exothermic while it is accompanied with an increase in the specific volume. This indicates that the d*P*/d*T* slope of the I-II equilibrium curve is negative. The convergence of the melting equilibrium lines at high pressure lead to a topological *P*-*T* diagram in which polymorph I possesses a stable phase region at high pressure. Thus, forms I and II are monotropically related at ordinary pressure and turn to an enantiotropic relationship at high pressure. Given that polymorph I is the densest form, it negates the rule of thumb that the densest form is also the most stable form at room temperature, similar to the case of paracetamol.

Keywords: polymorph, thermodynamics, phase diagram, heat capacity, stability, and specific volume

1 INTRODUCTION

1.1 THE EXCEPTIONAL DIFFERENCE BETWEEN THE MELTING POINTS OF THE TWO POLYMORPHS OF SPIRONOLACTONE

Most crystalline polymorphs of molecular compounds possess melting points that differ from each other by only a few degrees. Differences of more than fifty degrees are very rare, as can be inferred from a compilation of 103 sets of polymorphic systems involving "pharmaceuticals and other molecular compounds" by Burger and Ramberger (Burger and Ramberger, 1979b) in addition to more recent cases, which have been compiled in Table 1. In Figure 1, it is shown that about 56 % of these systems exhibit differences between their melting temperatures smaller than 10 K, and only fifteen cases (≈5%) exhibit differences higher than 40°C, which on closer scrutiny occurs mainly between the more stable polymorph and a polymorph ranking fourth or fifth in metastability.

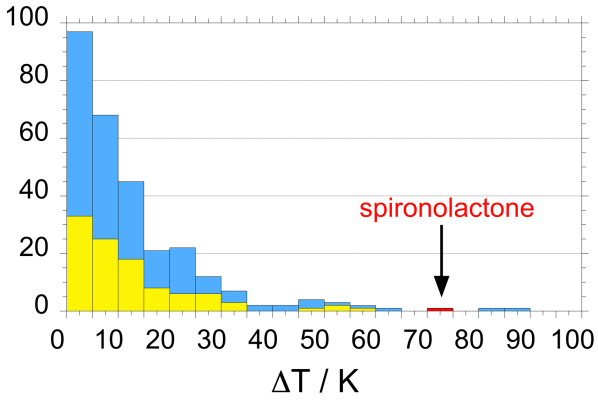

Figure 1. Number of polymorph pairs as a function of the temperature difference (ΔT) between the melting temperature of the most stable polymorph and a metastable one compiled by Burger and Ramberger in yellow (Burger and Ramberger, 1979b) and more recent data in blue (see also Table 1). ΔT is smaller than 15 K for 75% of the pairs and only 2 pairs (less than 1%) exhibit a difference of more than 80°C in melting points. The melting difference of spironolactone is marked in red.

The dimorphic system involving the orthorhombic forms of spironolactone, form I (Dideberg and Dupont, 1972) and form II (Agafonov et al., 1989), appear to exhibit a difference of more than 70 degrees in their melting temperatures, making it therefore an exceptionally uncommon case of crystalline polymorphism (Espeau et al., 2007). Form I melts and recrystallizes into form II in the temperature interval of 373-393 K. Form II, however, only melts at 480-483 K.

With such a large difference in melting points, it is rather puzzling why form I appears at all and the question arises whether form I has a stable domain in the pressure-temperature phase diagram, either at low temperature or at high pressure. For high-pressure measurements, a special analyzer developed in-house in the UPC (Barcelona) would have been a useful tool, however, the melting point of form II falls outside of its temperature range and the signals of the other transitions are too weak to be observed with sufficient precision. Therefore, using calorimetric and crystallographic data available in the literature and new experimental results obtained under ordinary pressure[1], a topological pressure-temperature phase diagram has been constructed involving spironolactone polymorphs I and II and its liquid phase.

[1] With ordinary pressure is meant that the system is not subjected to a pressure, but allowed to determine its own equilibrium pressure.

Table 1. Melting point differences between polymorphs of the same compound since the publication of Burger and Ramberger (Burger and Ramberger, 1979b)

		T_{fus}(i)/K	T_{fus}(j)/K	ΔT	Ref.
1	metacetamol	420.5 (I) 420.6 (I)	400 (II) 399.4 (II)	20.5 21.2	(McGregor et al., 2015) (Barrio et al., 2017a)
2	Racemic m-nisoldipine	408.95 410.94	402.4 403.31	6.5 7.63	(Yang et al., 2012) (Yang et al., 2013)
3	Apatinib mesylate	469.56	462.84	6.72	(Zhu et al., 2016)
4	Olopatadine HCl	526.12	523.19	2.93	(Laszcz et al., 2016)
5	nimesulide	422.4	419.8	2.6	(Barrio et al., 2017c)
6	Racemic Fluoxetine nitrate	385	383	2	(Carvalho Jr et al., 2016)
7	Acedapsone	565.95 (I) 565.95 (I)	556.65 (III) 561.85 (II)	9.3 4.1	(Bolla et al., 2014)
8	Cimetidine	426 (B) 426 (B)	419.5 (D) 423.5 (A)	6.5 2.5	(Shibata et al., 1983)
9	Ranitidine	350.84 (II)	346.65 (I)	4.19	(De Armas et al., 2009)
10	Ranitidine HCl	410.95 (2)	408.75 (1)	2.2	(Mirmehrabi et al., 2004)
11	Ticagrelor	422 (I) 422 (I)	402.5 (III) 410.5 (II)	19.5 11.5	(Bohlin, 2007)
12	4'-hydroxyacetophenone	381.9 (I)	377.2 (II)	4.7	(Joseph et al., 2017)
13	3,3'-Diindolylmethane	440 (II)	436 (I)	4	(Latosinska et al., 2016)
14	m-aminobenzoic acid	451.13 (II)	445.19 (I)	5.94	(Svard et al., 2010)

15	SSR180711C	448.0 (I)	446.7 (II)	1.3	(Robert et al., 2016)
16	Piracetam	426 (I)	412 (III)	14	(Céolin et al., 1996)
17	Rotigotine	370 (II)	350 (I)	20	(Rietveld and Ceolin, 2015)
18	FK664	413 (B)	388 (A)	25	(Miyamae et al., 1991)
19	Ritonavir	398.15 (II)	395.15 (I)	3	(Chemburkar et al., 2000)
20	Rimonabant	429.2 (II)	428.3 (I)	0.9	(Perrin et al., 2013)
21	Bicalutamide	465.6 (I)	462.9 (55)	2.7	(Gana et al., 2013)
22	Benfluorex HCl	433.64 (I)	427.48 (II)	6.16	(Maccaroni et al., 2010)
23	Biclotymol	400.5 (I)	373.8 (II)	26.7	(Ceolin et al., 2008)
24	Fananserine	375.1 (II) 375.1 (II) 375.1 (II)	366.3(I) 374.8 (III) 372.8 (IV)	8.8 0.3 2.3	(Giovannini et al., 2001)
25	Aprepitant	526.75 (I)	526.15 (II)	0.6	(Braun et al., 2008b)
26	*N*-Picryl-*p*-toluidine	439.25 (Ig)	436.65 (IIo)	2.65	(Braun et al., 2008a)
27	Aripiprazole	421.65 (I) 421.65 (I) 421.65 (I)	408.15 (IV) 416.15 (II) 412.35 (III)	13.55 5.5 9.3	(Braun et al., 2009)
28	Nembutal	402.65 (I) 402.65 (I) 402.65 (I)	382.15 (IV) 399.15 (II) 387.15 (III)	20.5 3.5 15.55	(Rossi et al., 2012)
29	Methylparaben	399.15 (1-I) 399.15 (1-I)	380.15 (1-107) 385.15 (1-112)	19 14	(Gelbrich et al., 2013)

		399.15 (1-I)	382.15 (1-III)	17	
30	7-Hydroxyisoflavone	488.15(II)	482.75 (I)	5.4	(Gong et al., 2016)
31	Irganox 1076®	324.15 (I) 324.15 (I) 324.15 (I)	278.45 (IV) 324.05 (II) 320.35 (III)	45.7 0.1 3.8	(Saunier et al., 2010)
32	Lifibrol	415 (I)	408 (II)	7	(Burger and Lettenbichler, 2000)
33	Praziquantel	415.71 (A)	385.25 (B)	30.46	(Zanolla et al., 2018)
34	Albendazole	493 (I)	433 (II)	60	(Pranzo et al., 2010)36
35	Theophylline	546.55 (I)	542.25 (II)	4.3	(Suzuki et al., 1989)
36	Atomoxetine HCl	441.05 (I)	437.45 (II)	3.6	(Stephenson and Liang, 2006)
37	Bentazon	413 (II) 413 (II)	400 (III) 405 (I)	13 8	(Braga et al., 2014)
38	Felodipine	418.05 (III) 418.05 (III)	407.05 (I) 414.70 (II)	11 3.35	(Srcic et al., 1992)
39	Auranofin	389 (B)	385 (A)	4	(Lindenbaum et al., 1985)
40	MK571	437 (I)	425 (II)	12	(Ghodbane and Mccauley, 1990)
41	WIN 63843 (pleconaril)	337.65 (I)	334.35 (III)	3.3	(Rocco and Swanson, 1995)
42	Sulfapyridine	459.45 (I)	450.45 (II)	9	(Bottom, 1999)
43	Benzidine	401 (II)	397 (I)	4	(Rafilovich and Bernstein, 2006)
44	Buspirone HCl	476.75 (2)	462.95 (1)	13.8	(Sheikhzadeh et al., 2006)
45	Cilostazol	432.0 (A)	408.8 (B)	23.2	(Stowell et al., 2002)

		432.0 (A)	419.0 (C)	13	
46	Curcumin	450.72 (1) 450.72 (1)	441.44 (3) 445.10 (2)	9.28 5.62	(Sanphui et al., 2011)
47	Diniflusal	486.30 (D) 486.30 (D)	485.45 (B) 485.95 (A)	0.85 0.35	(Perlovich et al., 2002)
48	Donepezil	367.39 (F) 367.39 (F) 367.39 (F)	362.42 (C) 363.82 (I) 367.09 (II)	4.97 3.57 0.30	(Park et al., 2013)
49	Doxazosin mesylate	551.05 (A) 551.05 (A) 551.05 (A) 551.05 (A)	501.1 (D) 549.65 (F) 543.95 (G) 531.15 (H) 548.05 (I)	49.95 1.40 7.1 19.9 3	(Grcman et al., 2002)
50	Famotidine	440.05 (A)	432.05 (B)	8	(Lu et al., 2007)
51	Florfenicol	427.5 (B)	425.45 (A)	2.05	(Sun et al., 2014)
52	Fluconazole	412.85 (A)	412.05 (B)	0.8	(Gu and Jiang, 1995)
53	Racemic flurbiprofen	386.65 (I) 386.65 (I)	360.10 (III) 365.15 (II)	26.55 21.5	(Henck and Kuhnert-Brandstatter, 1999)
54	Formoterol fumarate	423 (B) 423 (B)	396 (C) 400 (A)	27 20	(Jarring et al., 2006)
55	Ibopamin	408.39 (I)	403.85 (II)	4.54	(Laine et al., 1995)
56	Lamivudine	451 (II)	408 (I)	43	(Jozwiakowski et al., 1996)
57	Linezolid	453 (IV)	428 (II)	25	(Maccaroni et al., 2008)
58	Malotilate	335 (B)	325 (A)	10	(Vega and Baggio, 1989)
59	Metazachlor	356 (I)	338 (V)	18	(Griesser et al.,

		356 (I) 356 (I) 356 (I)	353 (II) 349 (III) 346 (IV)	3 7 10	2004)
60	Metoclopramide HCl	460 (I)	428 (II)	32	(Mitchell, 1985)
61	Nateglinide	447.25 (S) 447.25 (S)	402.35 (B) 411.05 (H)	44.9 36.2	(Bruni et al., 2009)
62	Nicardipine Hydrochloride	457 (α)	438 (β)	19	(Moreno-Calvo et al., 2011)
63	RS-Nitrendipine	430 (I) 430 (I)	398 (III) 405 (II)	32 25	(Burger et al., 1997)
64	Pemetrexed Diacid	408.43 (1)	397.32 (2)	11.11	(Michalak et al., 2015)
65	Piperine	405.64 (I) 405.64 (I)	389.63 (III) 401.12 (II)	16.01 4.52	(Pfund et al., 2015)
66	Piretanide	500 (A)	486 (B)	14	(Chikaraishi et al., 1994)
67	Piroxicam	475.75 (I)	472.85 (II)	2.9	(Vrecer et al., 2003)
68	Premafloxacin	471 (III) 471 (III)	416 (I) 439 (II)	55 32	(Schinzer et al., 1997)
69	Salicaine hydrochloride	429.15 (I)	425.35 (II)	3.65	(Schmidt et al., 2006)
70	Salmeterol Xinafoate	410.75 (II)	395.85 (I)	14.9	(Tong et al., 2001)
71	Sofosbuvir	395.37 (B)	393.89 (A)	1.48	(Qi et al., 2015)
72	Sulindac	460 (I)	456(II)	4	(Tros de Ilarduya et al., 1997)
73	Tegafur	448 (γ)	438 (δ)	10	(Uchida et al., 1993)
74	Telmisartan	542 (A)	456 (B)	86	(Dinnebier et al., 2000)
75	Temazepam	433.85 (O)	411.65 (VI)	22.2	(Jetti et al.,

		433.85 (O)	432.45 (X)	1.4	2011)
76	Terazosin hydrochloride	544.15 (II) 544.15 (II) 544.15 (II)	540.45 (I) 543 .55 (IV) 541.65 (III)	3.7 0.6 2.5	(Bauer et al., 2006)
77	Terfenadine	422 (I) 422 (I) 422 (I)	416.5 (IV) 421 (II) 418 (III)	5.5 1 4	(Leitao et al., 2002)
78	Racemic thalidomide	548.35(β) 549.75 (β)	545.45 (α) 548.65 (α)	2.9 1.1	(Reepmeyer et al., 1994) (Lara-Ochoa et al., 2007)
79	Tolbutamide	401 (I^H) 400.3 (I^H)	390 (II) 375.73 (V)	11 24.57	(Thirunahari et al., 2010) (Svard et al., 2016)
80	Tulobuterol	364 (1)	354 (2)	10	(Caira et al., 2004a)
81	Varenicline L-tartrate	497.15 (A)	489.05 (B)	8.1	(Murphy et al., 2010)
82	Stavudine	441.25 (I)	438.65 (II)	2.6	(Lu and Rohani, 2009)
83	Chenodeoxycholic acid	439 (I)	392 (III)	47	(Oguchi et al., 2003)
84	ASP3026	453 (A04) 453 (A04)	433 (A01) 443 (A03)	20 10	(Takeguchi et al., 2015)
85	Benoxaprofen	466 (II)	460 (I)	6	(Umeda et al., 1984)
86	HOKU-81	454 (II)	452 (I)	2	(Saito et al., 1983)
87	Tulobuterol HCl	443 (II) 443 (II)	422 (III) 436 (I)	21 7	(Saito et al., 1982)
88	(R,S)-Propranolol HCl	439 (I)	436(II)	3	(Bartolomei et al., 1998)

89	*m*-anisic acid	378.55 (I)	367.15 (II)	11.4	(Pereira-Silva et al., 2015)
90	Ambroxol	372.65 (I)	365.55 (II)	7.1	(Caira et al., 2004b)
91	Racemic betaxolol	342.15 (I)	306.55(II)	35.6	(Maria et al., 2013)
92	Bromopride	428 (I)	376 (II)	52	(Carrer et al., 2016)
93	Bisoprolol fumarate	378.65 (I)	369.75 (II)	8.9	(Detrich et al., 2018)
94	Delapril HCl	452.75 (D1)	438.15 (D2)	14.6	(Todeschini et al., 2014)
95	Manidipine HCl	494.05 (M1)	492.05 (M2)	2	(Todeschini et al., 2014)
96	Febantel	397.05 (I)	387.55 (II)	9.5	(Bruni et al., 2017)
97	Prilocaine HCl	442 (I)	438.5 (II)	3.5	(Schmidt et al., 2004)
98	*p*-Methylchalcone	369.45 (I)	362.55 (II)	6.9	(Barsky et al., 2008)
99	Nabumetone	353 (I)	338(II)	15	(Price et al., 2002)
100	Metaxalone	395.35 (B)	395.05 (A)	0.3	(Aitipamula et al., 2011)
101	Etiracetam	392.39 (II)	385.44 (I)	6.95	(Herman et al., 2011)
102	Cefamandole nafate	442.5 (IV)	437.0 (V)	5.5	(He et al., 2016)
103	Risperidone	443.26	435.25	8.01	(Pfeiffer, 2003)
104	3,3'-dihydroxy-β,β-carotene-4,4'-dione	503 (I)	489 (II)	14	(Guo and Ulrich, 2010)
105	Neotame	385 (G) 385 (G)	365 (A and F) 367 (D)	20 18	(Dong et al., 2002)
106	Imatinib mesylate	499 (α)	490 (β)	9	(Grillo et al., 2012)

107	NCX4016	335 (I)	328.3 (II)	6.7	(Foppoli et al., 2004)
108	Succinobucol	430 (A) 430 (A) 430 (A)	408.6 (E) 420.7 (C) 413.2 (D)	21.4 9.3 16.8	(Jurcek et al., 2012)
109	Alprazolam	500.17 (III)	495.15 (I)	5.02	(De Armas et al., 2007)
110	Nortryptiline HCl	490.1 (α)	490.0 (β)	0.1	(Vladiskovic et al., 2012)
111	Febuxostat	482.89 (I) 482.89 (I)	474.19 (III) 476.30 (II)	8.70 6.50	(Patel et al., 2015)
112	Carnidazole	418.25 (I)	411.05 (II)	7.2	(De Armas et al., 2006)
113	Nicergoline	407 (I)	394 (II)	13	(Malaj et al., 2011)
114	E2101	421.25 (I)	412.95 (II)	8.3	(Kushida and Ashizawa, 2002)
115	Celecoxib	434	421	13	(Lu et al., 2006)
116	Piroxicam pivalate	426.95 (1)	409.65 (2)	17.3	(Giordano et al., 1998)
117	LY334370 HCl	547 (I) 547 (I)	463 (II) 538 (III)	84 9	(Reutzel-Edens et al., 2003)
118	Clopidogrel Bisulfate	454.35 (I)	449.25 (II)	5.1	(Khomane et al., 2012)
119	Irganox 3114®	492 (I)	478 (II)	14	(Saunier et al., 2012)
120	Probucol	399 (I) 399 (I)	381 (III) 389 (II)	18 10	(Kawakami and Ohba, 2017)
121	Suplatast tosilate	359.85 (α) 359.85 (α) 359.85 (α) 359.85 (α)	347.95 (δ) 359.65 (γ) 356.15 (η) 351.25 (ζ)	11.9 0.2 3.7 7.9	(Nagai et al., 2014)

		359.85 (α)	348.35 (ε)	11.5	
122	Sitafloxacin	513 (α)	493 K (β)	20	(Suzuki et al., 2010)
123	L-arabitol	374 (I)	353 (II)	21	(Carpentier et al., 2013)
124	Amisulpride	398.45 (I)	395.85 (II)	2.6	(Zhang and Chen, 2017)
125	Ciprofloxacine Saccharinate	573.95 (I)	567.45 (II)	6.5	(Singh and Chadha, 2017)
126	DuP 747	491.3 (II)	483.6 (I)	7.7	(Raghavan et al., 1994)
127	(-)-*N*-Methylephedrine	360.8 (I)	359.6 (II)	1.2	(Tulashie et al., 2016)
128	Venlafaxine HCl	483.99 (1) 491.97 (6)	481.21 (2) 481.55 (1)	2.78 10.42	(Roy et al., 2005) (Roy et al., 2007)
129	Venlafaxine	351.25 (III) 351.25 (III)	348.05 (I) 349.65 (II)	3.2 1.6	(van Eupen et al., 2009)

1.2 AVAILABLE DATA FROM LITERATURE

Spironolactone ($C_{24}H_{32}O_4S$ with M = 416.57 g mol^{-1}) is an aldosterone agonist used in human therapeutics as a diuretic. The suspicion of spironolactone polymorphism arose about 50 years ago due to infrared spectroscopic measurements (Mesley and Johnson, 1965). In 1972, the crystal structure of a polymorph grown from an acetone solution was solved and thus called form I (Dideberg and Dupont, 1972). With differential scanning calorimetry (DSC), it was observed that spironolactone crystallized from ethanol or from water exhibited a small exothermic peak at about 433 K and an endothermic peak at about 483 K, whereas spironolactone crystallized from methanol exhibited an endothermic peak at about 393 K followed by an exothermic peak at about 413 K (Sutter and Lau, 1975). These and other literature data have been compiled in Table 2. Below follows a summary description of the findings in the literature.

In 1976, Florence and Salole demonstrated that pre-melting behavior observed by DSC was radically altered by grinding (Florence and Salole, 1976). They subjected a commercial specimen to differential thermal analysis (DTA) at a 10 K min^{-1} heating rate and recorded an endothermic peak (onset at about 423 K) followed by an exothermic peak (onset at about 433 K) and a melting peak at about 483 K (Florence and Salole, 1976). Unfortunately, no X-ray data was reported, making it difficult to link the observed thermal behavior to a specific polymorph. In the 1980s, further investigations into the solid state of spironolactone were carried out confirming the existence of multiple polymorphs in addition to a number of solvates (Eldalsh et al., 1983; Salole and Alsarraj, 1985a, b). In the early 1990s, the polymorphism of spironolactone and its solvation was revisited

by Agafonov et al. (Agafonov et al., 1991a; Agafonov et al., 1991b), who previously had solved the crystal structure of a second polymorph (thus named form II) using crystals grown from an acetone solution (Agafonov et al., 1989). Berbenni et al. found melting temperatures ranging from 480 to 486 K and melting enthalpies from 44 to 54 J g^{-1} obtained from four solvent-free samples; however, their different X-ray powder diffraction patterns were not indexed and the samples were listed as polymorphs 'M', 'EV', 'E' and 'A', respectively (Berbenni et al., 1999). Moreover, Berbenni et al. and Marini et al. reported that spironolactone decomposes in the melt (Berbenni et al., 1999; Marini et al., 2001), which obviously may affect the values of the melting enthalpies and the melting point of form II.

In 2003, high resolution X-ray powder diffraction experiments as a function of temperature demonstrated that form II exhibits no structural change up to its fusion, whereas form I transforms into form II in the 373 – 398 K temperature interval (Liebenberg et al., 2003). In 2007, a I→II transformation was observed with an onset in the 373 – 393 temperature interval and with a liquid as an intermediate phase, which was interpreted as a melting recrystallization (Espeau et al., 2007). Summing over the complete endo-exothermic effect resulted in a value of 0 ± 2 J g^{-1} for the enthalpy of the I→II transition at the temperature of fusion of form I leaving the relative enthalpy ranking between the two phases undetermined (Espeau et al., 2007). The melting enthalpy of form II, $\Delta_{II \rightarrow L}H$ = 55 J g^{-1} at 480 K (onset), was found to be close to previous values. In addition, specific volumes of forms I, v_I, and II, v_{II}, were determined as a function of temperature in the range from room temperature up to their respective melting points (Espeau et al., 2007). At 300 K, those equations lead to the specific volumes v_I (300 K) = 0.78942 cm^3 g^{-1} and v_{II} (300 K) = 0.80099 cm^3 g^{-1}, which clearly demonstrates that form I is denser than form II. Fukuoka et al. in 1991 found a glass transition for spironolactone at T_g = 331 K (Fukuoka et al., 1991), rather different from the value of 364 K reported by Mahlin and Bergström in 2013 (Mahlin and Bergstrom, 2013).

There is no doubt that the phase behavior of spironolactone is challenging to study and except for the melting of form II uncertainty exists about the rest of its phase behavior. Seventy degrees of difference appears to exist between the melting temperatures of forms I and II and still form I can be easily obtained experimentally. Moreover, as can be judged from the specific volumes, form I is the densest polymorph and clearly less stable than form II; this is in obvious contradiction with the density rule proposed by Burger and Ramberger (Burger and Ramberger, 1979a, b). In the present paper an attempt will be made to shine some light on the phase behavior of spironolactone by constructing a pressure-temperature phase diagram. Most likely, the last word is not written about the exact calorimetric data of the phase behavior of spironolactone, but using data from the literature and additional measurements, it will be shown that despite the 70 degrees of difference in melting points, form I does possess a stable domain in the pressure-temperature phase diagram.

Table 2. Calorimetric data on spironolactone in the literature [a]

T_g /K	$T_{I\rightarrow II}$ /K	$T_{I\rightarrow L}$ /K	T_{cryst} /K	$T_{II\rightarrow L}$ /K	$\Delta_{I\rightarrow II}$ H /Jg^{-1}	$\Delta_{I\rightarrow L}$ H /Jg^{-1}	$\Delta_{II\rightarrow L}$ H /Jg^{-1}	reference
			433 (exo)	483				(Sutter and Lau, 1975)
	393?	393?	413 (exo)					(Sutter and Lau, 1975)
		423? [b]	433 (exo) [b]	483 [b]				(Florence and Salole, 1976)
		478?		483		48?	53	(Agafonov et al., 1991a; Agafonov et al., 1991b)
				480-486			44-54	(Berbenni et al., 1999)
							50.8 ±1.5	(Marini et al., 2001)
				480			51.93	(Pisegna, 1999)
	373-398 (Xr)							(Liebenberg et al., 2003)
				481.15			51.3 ±1.3	(Snider et al., 2004)
	373-393?	373-393?		480	0 ±2		55	
				475-476[c]			35.79-51.86 [c]	(Brandão et al., 2008)
				481			54.1	(Dong et al., 2009)
			453-473 [d]	476.5 [d]			44.5 [d]	(Dong et al., 2009)
331								(Fukuoka et al., 1991)
364				486			60	(Mahlin and Bergstrom, 2013)

				481.57			49.58	(Zhang et al., 2014)
				481.9-483.1			49.58-50.82	(Jiang et al., 2015)
				475.9			45.2	(De Resende et al., 2016)

[a] Transitions are endothermic unless otherwise specified, transition temperatures are obtained by DSC unless otherwise specified (Xr: X-ray diffraction), values of which the interpretation is not clear or in doubt are marked with a question mark.

[b] ground sample

[c] microparticles

[d] "micrometer sized nanoparticles" [sic] (Dong et al., 2009)

2 MATERIAL AND METHODS

2.1 SAMPLE OF FORMS I AND II

Samples of medicinal grade from Sanofi (France) and from Welding GMBH (Germany), purity > 99%, were respectively found to consist of pure form II and pure form I by X-ray diffraction and used as such. In addition, crystals of form I were grown by evaporating solutions of form II in ethanol at room temperature, in accordance with the method described previously (Nicolai et al., 2007). A thermogravimetric curve of the latter form I has been provided in the supplementary materials, Figure S2.

2.2 HIGH RESOLUTION X-RAY POWDER DIFFRACTION

High-resolution X-ray diffraction patterns were recorded at room temperature with cylindrical position-sensitive detectors (CPS120) from INEL (France) using monochromatic Cu-Kα_1 (λ = 1.54061 Å) radiation. Figure 2 demonstrates that the experimental diffraction patterns exhibit no differences with the respective calculated patterns based on the crystal structures.

2.3 DIFFERENTIAL SCANNING CALORIMETRY

Temperatures and heats of fusion were determined at various heating rates with a TA-Instruments Q100 thermal analyzer. Indium (T_{fusion} = 429.75 K, $\Delta_{fusion}H$ = 28.45 J g^{-1}) was used as a standard for temperature and enthalpy calibration.

Specific heat capacities as a function temperature were determined with the TA-Instruments Q100 using a modulated signal by superimposing a sinusoidal temperature change on the linear temperature increase. The linear heating rate was 2 K min^{-1} while the superimposed sinusoidal had an amplitude of $\pm$ 0.5 K and a period of 60 s. Vitreous spironolactone was obtained after heating specimens at 100 K min^{-1} up to 490 K and quenching them to room temperature within a few seconds to avoid decomposition. The so-obtained colorless transparent glass was ground into a powder and subjected to modulated DSC experiments from 220 K to 430 K.

Samples were weighed using a microbalance sensitive to 0.01 mg and sealed in aluminum pans.

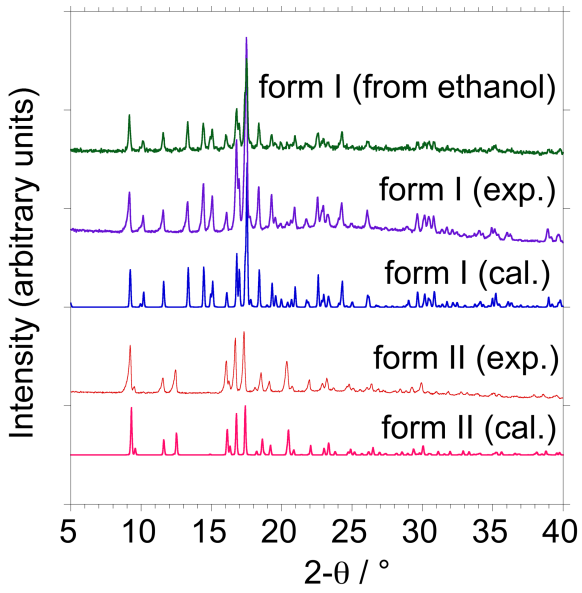

Figure 2. High-resolution X-ray powder diffraction patterns of spironolactone forms I and II: exp: experimental pattern at 300 K with form I from Welding and form II from Sanofi, ethanol: sample from Sanofi recrystallized into form I, cal = calculated pattern based on the crystallographic information files (CIF) from the Cambridge Structural Database (CSD) with registry codes: form I = ATPRCL10, form II = ATPRCL01.

3 RESULTS

3.1 CALORIMETRIC DATA

For comparison with the melting data from the literature (Table 2), DSC measurements with 15 separate samples of form II were carried out (Table 3) demonstrating that the present sample of form II melts at 479.6 ± 0.6 K with a melting enthalpy of $\Delta_{II\rightarrow L}H$ = 54.0 ± 1.5 J g^{-1} (22.49 ± 0.62 kJ mol^{-1}) i.e. close to the previously reported values of 480 K and 55 J g^{-1}, respectively, in reference (Espeau et al., 2007).

Form I was obtained from the Sanofi batch by evaporating an ethanol solution and its transformation behavior is represented by curve 3 in Figure 3. Part 'a' of the convoluted phenomenon 'ab' is the onset of the melting of form I, however, it is taken over half way by the recrystallization of form II (part 'b'). This behavior has been reported previously in the literature, however at that time it could not be determined whether the I→II transformation had a positive or a negative enthalpy (Espeau et al., 2007). In the present case, summation over the endo-exothermic effect (peaks 'a' and 'b' in Fig. 3) results in $\Delta_{I\rightarrow II}H$ values ranging from +2.1 to -11.7 J g^{-1} depending on the run and the mean over 7 values is −4.3 ± 4.0 J g^{-1} with all enthalpy values except for one being negative (Table 3). The mean onset temperature of fusion of form I, peak 'a', is $T_{I\rightarrow L}$ = 408 ± 3 K (see Table 3).

Whereas form I of the spironolactone batch from Sanofi consistently melted before recrystallization into form II, form I from Welding exhibited a single exothermic peak with a mean enthalpy change of −6.9 ± 0.3 J g^{-1} and at a mean temperature of 375 ± 3 K (see curve 2 in Figure 3 and Table 4). The single exothermic peak represents a direct transformation of form I into form II and confirms beyond doubt ($\Delta_{I\rightarrow II}H$ = −6.9 ± 0.3 J g^{-1}) that the transition of form I into form II has a negative enthalpy change.

The glass transition temperature T_g was found to be at 306 K in the present series of experiments, as can be seen in the inset of Figure 3. This temperature is near the value of 320 K found with the empirical formula by Tammann: T_g = 2/3 T_{fus}.

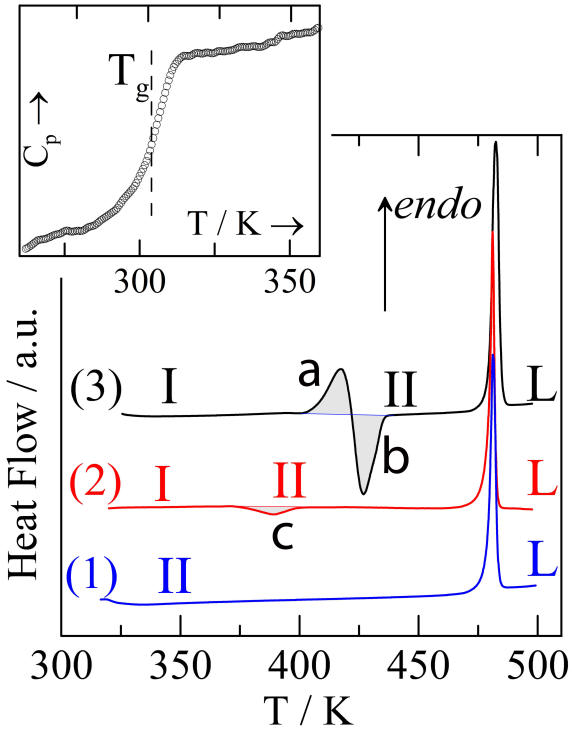

Figure 3. DSC curves with (1) the melting curve of commercial spironolactone form II, (2) the irreversible (exothermic) transition of spironolactone form I to form II (sample from Welding), and (3) the same transition through a melting (**a**)-recrystallization (**b**) process (sample from Sanofi). Area '**b**' is found to be greater than area '**a**', leading to a negative value for the transition enthalpy of form I to form II, as confirmed by negative area '**c**'. Inset: glass transition observed at 306 K by reheating the glass obtained from the melt.

Table 3. Onset temperatures and enthalpies of phase transitions obtained with the spironolactone sample from Sanofi[a]

Initial form	Heating rate /K min^{-1}	$T_{I\rightarrow L}$/K[b]	$\Delta_{I\rightarrow II}H$[c] /J g^{-1}	$T_{II\rightarrow L}$/K	$\Delta_{II\rightarrow L}H$ /J g^{-1}
I	15	406.7	-11.7	479.8	54.3
I	20	408.2	-4.7	480.6	52.7
I	25	407.7	-3.8	479.7	53.9
I	30	408.1	-3.9	480.0	54.2
I	35	410.2	-4.1	479.9	54.7
I	40	403.4	-3.7	478.4	53.6
I	45	412.1	+2.1	480.3	53.3
I	15	405.6	-	479.8	58.3
II	15			479.2	53.2
II	20			478.5	53.2
II	25			478.8	56.1

II	30			479.6	52.5
II	35			479.3	54.6
II	40			479.7	52.9
II	45			479.8	53.1
Mean values (standard deviation)		408 ± 3	-4.3 ± 4.0	479.6 ± 0.6	54.0 ± 1.5

[a] The commercial form is form II, form I was prepared by evaporating an ethanol solution at room temperature.
[b] The onset of the first transition peak in the Sanofi sample is related to the melting of form I, see Figure 3 for clarification.
[c] The overall enthalpy of the first transformation in the Sanofi sample is related to the combined conversion of form I into liquid and its recrystallization into form II, see Figure 3 for clarification.

Table 4. Calorimetric data (onset temperatures and enthalpies of phase changes) obtained with spironolactone form I from Welding

Sample	$T_{I\rightarrow II}$ /K	$\Delta_{I\rightarrow II}H$/J g^{-1}	$T_{II\rightarrow L}$ /K	$\Delta_{II\rightarrow L}H$/J g^{-1}
1	371.9	-6.2	-	-
2	370.5	-6.4	477.2	53.6
3	375.8	-7.3	479.5	55.0
4	375.9	-7.3	479.2	55.8
5	376.0	-7.2	479.4	53.5
6	379.2	-6.2	479.3	54.9
7	377.7	-7.3	479.5	54.8
Mean	375 $\pm$ 3	−6.9 $\pm$ 0.3	479.0 $\pm$ 1.0	54.6 $\pm$ 0.9

3.2 Specific Heats

The specific heats of form II and of the melt have been fitted in the temperature range of 250 K to 450 K and 325 K to 450 K respectively (See Supplementary Information), leading to:

$C_{p,II}$ / J g^{-1} K^{-1} = 0.2148(43) – 1.502(25) ×10^{-3} T/K + 4.186(36) ×10^{-6} (T/K)^2 (r^2 = 0.9990) (1)

$C_{p,L}$ / J g^{-1} K^{-1} = 0.2706(93) + 4.68(24) ×10^{-4} T/K (r^2 = 0.94) (2)

Using these equations and extrapolating to the melting point of form II at 479.6 K, the relative enthalpies of the liquid and of form II have been calculated as a function of the temperature (Figure 4).

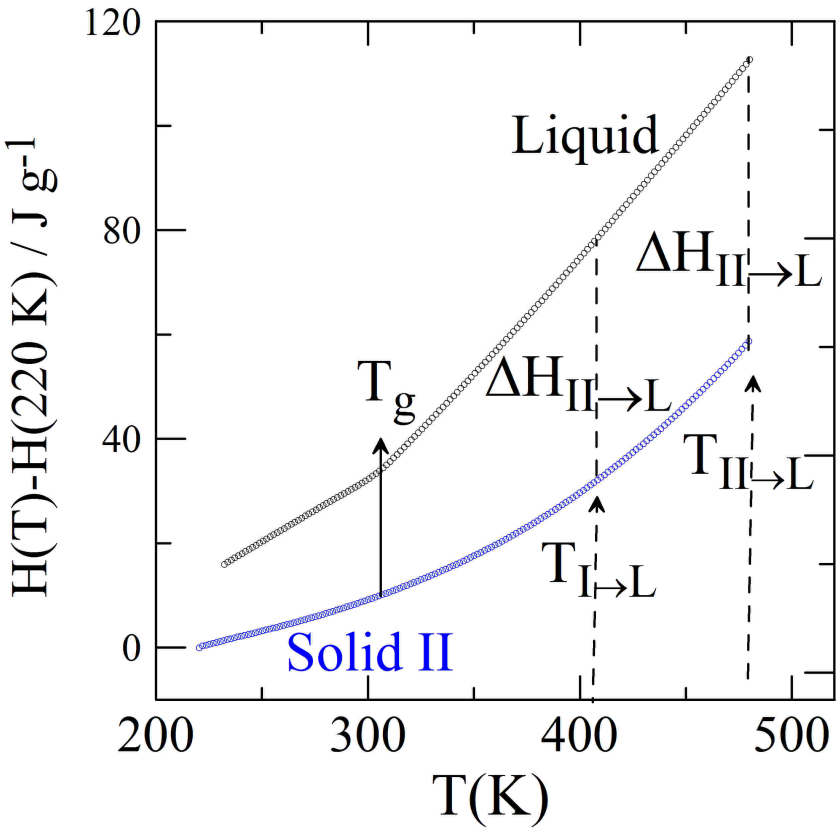

Figure 4. The relative enthalpy of form II and of the liquid obtained by numerical integration of the heat capacity data.

4 Discussion – Interpretation of the results through a pressure-temperature phase diagram

4.1 Global evaluation of the data and the phase behavior of spironolactone

It is clear from the introduction and the results that the phase behavior of spironolactone is not easy to understand. Based on the present batches from Sanofi and Welding, one can consider that the melting point and melting enthalpy of form II are reasonably correctly defined by the mean values in Table 3. The temperature of fusion for form I possesses a larger uncertainty, but it can be considered to be in the order of 408 ± 3 K. Obviously, the enthalpy of fusion for form I is experimentally inaccessible as the melting peak and the recrystallization peak are convoluted (Figure 3); however, an estimate of this value will be calculated below in the discussion. Finally, the enthalpy difference between forms I and II is found equal to −6.9 ± 0.3 J g^{-1}, although in terms of accuracy, it is probably in the order of −6.9 ± 1 J g^{-1}.

Before constructing the topological phase diagram, the phase behavior will be evaluated using the Le Chatelier principle. The behavior of spironolactone in relation to the pressure can be deduced from the specific volumes of the two polymorphs (see introduction and (Espeau et al., 2007)). Form I is the denser polymorph and therefore its relative stability will increase with pressure, whereas the relative stability of form II will decrease. It implies that if a phase equilibrium exists, form I will be stable at the high-pressure side and form II at the low-pressure side. A similar analysis can be carried out in terms of the enthalpy of form I and form II. The data from Tables 3 and 4 indicate beyond reasonable doubt that form I possesses a higher absolute enthalpy than form II, which implies that form I is the high temperature form. Interestingly, it is form II that has the highest melting point and this leads to the immediate conclusion that any equilibrium between forms I and II will be located at

a higher temperature than the melting point of form II and thus this equilibrium will be metastable under normal pressure. Hence, without any mathematical calculation, it can be concluded that to accommodate the density and enthalpy requirements of the system, the I-II phase equilibrium line necessarily possesses a negative slope (see Figure 5) with form I stable above the equilibrium and form II below. Furthermore, it can be stated that this I-II phase equilibrium is located at positive pressures (P >> 0 MPa) to accommodate for the fact that form II exhibits the stable melting temperature. Finally, this leads to the conclusion that form II is the only stable form under ordinary conditions, i.e. the equilibrium between form II and the vapor phase is stable from 0 K up to its melting point (see Figure 5). This result implies that unless the data in the Tables 3 and 4 are substantially wrong, any calculated phase diagram must obey the overall layout dictated by the Le Chatelier principle as depicted in Figure 5.

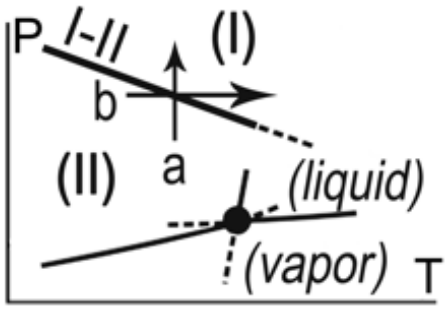

Figure 5. Schematic pressure-temperature phase diagram (not to scale) following the Le Chatelier principle applied to the data in Tables 1 and 2. Arrow "a" represents the transformation of form II into the denser form I on increasing pressure and arrow "b" represents the endothermic transformation of form II into form I, which possesses the higher absolute enthalpy. The phase equilibrium between forms I and II must have a negative slope to accommodate a high-pressure, high-temperature phase I and a low-temperature, low-pressure phase II. As a result, form II is the only stable phase under ordinary conditions, i.e. the solid II – vapor equilibrium, up to its melting point (solid black circle). Solid lines: stable phase equilibria, dashed lines: metastable phase equilibria.

4.2 AN EQUATION DESCRIBING THE II-L EQUILIBRIUM

A mathematical expression for a two-phase equilibrium line can be obtained by using the Clapeyron equation and as the simplest expression for a monotonic function (Ceolin and Rietveld, 2017), a straight line can be used. The melting point of form II is the best-documented phase transition in the spironolactone system and the one that most of the literature data seem to agree upon. The data in Table 3 will be used, which is similar to the data in the literature discussed in the introduction. To calculate the slope of the II-L equilibrium with the Clapeyron equation, the volume change on melting is needed too, however, slow decomposition of spironolactone in the molten state prevented the direct measurement of the specific volume of the liquid, which necessitates high temperatures for considerable amounts of time. Nevertheless, several authors have reported mean values for the volume change on melting for organic molecular compounds. Ubbelohde found that the volume increase on melting ranges from 7 to 16 % with a mean value of 11.5 %, a volume increase that has been confirmed by Gavezzotti (Gavezzotti, 2013; Ubbelohde, 1965). This value is very close to the value of 12 % proposed by Goodman et al. and to the mean value of 10 % found within 6 and 17 % for several molecular solids of pharmaceutical interest (Céolin and Rietveld, 2015; Goodman et al., 2004; Rietveld and Céolin, 2015). It can be concluded that as an approximation, the volume change on melting of the highest melting polymorph can be taken as 11 % of its specific volume.

The specific volume of polymorph II at its melting point of 479.6 K can be calculated using data from Espeau et al. (Espeau et al., 2007) and leads to a value of 0.8291 cm^3g^{-1}. The volume change on melting is taken as 11 % of this value, which equals $\Delta_{II\rightarrow L}v$ = 0.0912 cm^3g^{-1}, which leads to 0.9203 cm^3g^{-1} for the value of the specific volume of the melt. With the volume change, the enthalpy change, $\Delta_{II\rightarrow L}H$ = 54.0 J g^{-1}, and the melting temperature, the slope in the pressure-temperature plane, dP/dT, for the two-phase equilibrium II-L can be calculated

resulting in 1.23 MPa K^{-1}. Using P = 0 MPa at $T_{II\to L}$ = 479.6 K, because the vapor pressure at the melting point is necessarily smaller than 1 atm (= 0.1 MPa), one can obtain a linear expression for the equilibrium between form II and the liquid as a function of pressure and temperature:

$$P_{II\text{-}L}/\text{MPa} = 1.23\ T/\text{K} - 592 \qquad (3)$$

4.3 AN EQUATION DESCRIBING THE I-L EQUILIBRIUM

To formulate a mathematical description for the I-L equilibrium line, its equilibrium temperature, the enthalpy change on melting and the volume change on melting are needed for the Clapeyron equation. The equilibrium temperature is the melting point reported in Table 3. The enthalpy change on melting or the heat of fusion will have to be calculated, making use of the heat capacity eqs. 1 and 2. In addition, for the volume change on melting, the specific volume of the melt needs to be determined. These two inequalities between form I and the liquid, $\Delta_{I\to L}H$ and $\Delta_{I\to L}v$, will be calculated below using a few approximations. Obviously, approximations will increase the incertitude over the accuracy of the final expression. Nonetheless, considering Figure 5, it is clear that the resulting expression for the I-L equilibrium should meet the II-L equilibrium at high pressure, because that is where the I-II and II-L equilibria meet (Figure 5). The intersection of I-II and II-L will result in the triple point I-II-L and this triple point is part of the I-L equilibrium too. It implies that the Clapeyron equation must result in a slope dP/dT < 1.23 MPa K^{-1}, the slope of the II-L equilibrium.

4.3.1 HEAT OF FUSION OF FORM I

The heat of fusion of form I can only be determined indirectly, because of the immediate recrystallization of its melt into form II (Sanofi sample) or its direct transformation into form II (Welding sample). It necessitates the use of the specific heats as provided by eqs. 1 and 2. First, the heat of fusion of form II is obtained at the melting point of form I, using the Kirchhoff equation:

$$\Delta_{II\to L}H(T_{I\to L}) = \Delta_{II\to L}H(T_{II\to L}) + \int_{T_{II\to L}}^{T_{I\to L}} \Delta_{II\to L}C_p\,dT \qquad (4)$$

in which $\int_{T_{II\to L}}^{T_{I\to L}} \Delta_{II\to L}C_p\,dT = \int_{T_{II\to L}}^{T_{I\to L}} (C_{p,L} - C_{p,II})\,dT$ is the change in the difference in enthalpy between form II and the liquid when going from the melting point of form II ($T_{II\to L}$) to the melting point of form I ($T_{I\to L}$). Using the data from Table 3, the respective melting points are $T_{II\to L}$ = 479.6 K and $T_{I\to L}$ = 408 K. The change in the enthalpy using eqs. 1 and 2 leads to $\int_{T_{II\to L}}^{T_{I\to L}} \Delta_{II\to L}C_p\,dT = -7.46\ \text{J g}^{-1}$ (See eqs. S.3-S.7 in the supplementary information). Taking into account the melting enthalpy of form II at its melting point, $\Delta H_{II\to L}$ ($T_{II\to L}$) = 54.0 J g^{-1}, the melting enthalpy of form II at the melting temperature of form I becomes $\Delta H_{II\to L}$ ($T_{I\to L}$) = 46.5 J g^{-1}.

The enthalpy of fusion of form I, $\Delta H_{I\to L}$, can be found using the property of a function of state that its value is only determined by the initial and final conditions and the path does not affect its value: $\Delta H_{I\to L} = \Delta H_{I\to II} + \Delta H_{II\to L}$ and thus $\Delta H_{I\to L}$ = (−6.9) + 46.5 = 39.6 J g^{-1}. The enthalpy change between form I and form II, $\Delta H_{I\to II}$, is here taken as −6.9 J g^{-1} (Table 4), as the change in the difference in the specific heat capacity between the two solids is expected to be small and $T_{I\to II}$ and $T_{I\to L}$ are relatively close.

4.3.2 SPECIFIC VOLUME OF THE LIQUID AS A FUNCTION OF THE TEMPERATURE

The specific volume of the melt at the melting point of form I is necessary to calculate the change in the specific volume on the melting of form I. Sufficiently far from the critical point, the temperature dependence of v_L is usually described by a straight line: $v_L = v_0 + (a_{v,L}\cdot v_0)\cdot T$ with v_0 the specific volume at T = 0 K and $a_{v,L}$ a measure for the slope relative to v_0. In the case of spironolactone, an approximation for this expression can be obtained by using the volume of the liquid at the melting point of form II (see the discussion above on the slope of the II-L equilibrium line) and statistical information on the difference in the specific volume between its glass and its crystalline solid at the glass transition temperature (T_g), the former being 6 % larger. Very few

data are available in the literature, however, a few glass – crystal volume differences obtained from experiment have been recently reported for a number of pharmaceuticals (see Table 5).

There is a large spread in the glass transition temperatures obtained for spironolactone. In the literature, values of 331 K (Fukuoka et al., 1991) and 364 K (Mahlin and Bergstrom, 2013) have been found, whereas in the present experiments T_g was found to be 306 K. Because the latter value was obtained together with the other data in Table 1 that have been used for the calculations, 306 K, will be used. For a higher T_g, the slope of the specific volume of the liquid, dv_L/dT, will be steeper and the specific volume of liquid spironolactone will be somewhat smaller at the melting point of form I, thus decreasing the volume difference between the solid and the liquid. Because the volume difference is found in the denominator of the Clapeyron equation, a smaller difference will make the slope of the I-L phase equilibrium steeper. Following the arguments in the first section of the discussion, the slope can never be larger than 1.23 MPa K^{-1}, as in that case the two phase equilibria I-L and II-L will intersect at negative pressure and that would invalidate the rather basic observations on which the phase diagram in Figure 5 is based.

Table 5. Volume changes of pharmaceuticals at melting points and glass transition temperatures obtained from experiment

	v_L/v_I at $T_{I\rightarrow L}$	$T_{I\rightarrow L}$ /K	v_L/v_I at T_g	T_g /K	Ref.
biclotymol	1.13	400.5	1.05	294	(Ceolin et al., 2008)
ternidazole	1.11	333.0	1.07	235	(Mahé et al., 2011)
morniflumate	1.12	348.1	1.06	249	(Barrio et al., 2017d)
Rimonabant	1.11	429.2	1.04	350	(Perrin et al., 2013)
Prilocaine	1.13	311.5	1.07	218	(Rietveld et al., 2013)
Paracetamol	1.15	442.3	1.07	298	(Espeau et al., 2005)

The specific volume of the melt at $T_{II\rightarrow L}$ is 0.9203 cm^3g^{-1} as determined above. If the specific volume of the glass at T_g is 6 % larger than the stable crystalline form, it can be calculated evaluating the specific volume of form II (Espeau et al., 2007) at T_g = 306 K leading to $v_{II}(T_g)$ = 0.8019 $cm^3\ g^{-1}$ and for the liquid at the glass transition v_L = 0.8500 $cm^3\ g^{-1}$. This data can be used to obtain a linear expression for the specific volume of the liquid as a function of the temperature:

$$v_L/\ cm^3g^{-1} = 0.726 + 4.05 \times 10^{-4}\ T/K \qquad (5)$$

4.3.3 An equation for the I-L equilibrium and triple point I-II-L

With eq. 5, v_L at $T_{I\rightarrow L}$ = 408 K is found to be 0.8913 $cm^3\ g^{-1}$. At this temperature, v_I equals 0.8034 $cm^3\ g^{-1}$ (Espeau et al., 2007), which leads to a volume change, $\Delta_{I\rightarrow L}v$ of 0.0879 cm^3g^{-1} on melting of form I. Using this volume difference together with $\Delta_{I\rightarrow L}H$ = 39.6 J g^{-1} at the I-L equilibrium temperature $T_{I\rightarrow L}$ = 408 K in the Clapeyron equation, the slope of the I-L equilibrium is found to be 1.11 MPa K^{-1}, which is indeed smaller than the slope of equilibrium II-L confirming that the two equilibria converge on increasing pressure and temperature. Setting the pressure P equal to 0 MPa at $T_{I\rightarrow L}$, a linear expression of the I-L equilibrium can be obtained:

$$P_{I\text{-}L}/MPa = 1.11\ T/K - 451 \qquad (6)$$

Using eqs. 3 and 6, the triple point coordinates of I-II-L are found to be $T_{I\text{-}II\text{-}L}$ = 1094 K and $P_{I\text{-}II\text{-}L}$ = 758 MPa.

In the case that 364 K is used as the glass transition temperature, which is the highest value found in the literature (Mahlin and Bergstrom, 2013), it would result in an expression for the I-L equilibrium of P = 1.23 T – 500 and the triple point would be found at T = 9875 K and P = 11600 MPa. This is obviously much larger than the triple point coordinates calculated with eq. 6, because for T_g = 364 K, the slope of the I-L equation becomes only a fraction smaller than the slope of II-L; nonetheless, it does not invalidate the schematic phase diagram based on the principle of Le Chatelier in Figure 5.

4.4 AN EQUATION FOR THE I-II EQUILIBRIUM LINE

As concluded in section 4.1, the slope dP/dT of the I-II equilibrium line is negative with form I stable above and on the right-hand side of the equilibrium line and form II stable below the equilibrium line and on its left-hand side. Because the triple point I-II-L obtained with eqs. 3 and 6 is rather high in pressure and temperature, it is not possible to obtain reliable calorimetric data on the I-II slope. A simple estimate can be obtained by considering that the enthalpy of transition $\Delta_{I\rightarrow II}H$ = −6.9 J g^{-1}. This enthalpy has been obtained at a temperature of 375 K, hence an estimate of the entropy involved is −0.018 J g^{-1} K^{-1}. Taking the volume difference between the two solid phases at this temperature leads to 0.0136 cm^3 g^{-1}. With the Clapeyron equation, these data result in a rough estimate of the slope of the I-II equilibrium of −1.4 MPa K^{-1}. This slope can be tentatively used to obtain an expression for the I-II phase equilibrium located at the I-II-L triple point (T = 1094 K and P = 758 MPa). It results in the following estimate for the I-II phase equilibrium:

$$P_{I\text{-}II}/\text{MPa} = -1.36\ T/\text{K} + 2241 \qquad (7)$$

With this last equation, the complete topological phase diagram of the two solid phases of spironolactone can be described (Figure 6).

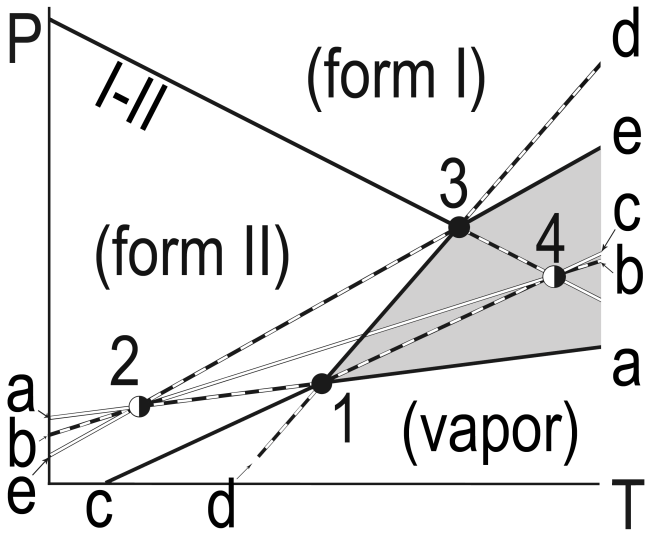

Figure 6. Topological pressure-temperature phase diagram of spironolactone indicating the relative positions of the stable phase regions of forms I and II, the vapor (V) and the liquid (L). The liquid domain is shown in grey. Triple points: 1= II-L-V, 2 = I-L-V, 3 = I-II-L, 4 = I-II-V. Two-phase equilibrium lines: aa = L-V, bb = I-V, cc = II-V, dd = II-L and ee = I-L. Stability ranking of the two-phase equilibria (lines) and the triple points (circles): Black = stable, black and white = metastable, white = supermetastable.

5 CONCLUDING REMARKS

The topological pressure-temperature phase diagram of spironolactone describing the phase relationships between forms I and II of spironolactone is presented in Figure 6. As stated in the beginning of the discussion, the I-II equilibrium line is located at high pressure. The only stable phase of importance for drug formulations is form II, which is stable over the entire temperature range under ordinary pressure (solid line c – 1 in figure 6).

The phase diagram in Figure 6 has not been easily obtained, because the transformation of form I into form II through the liquid phase was difficult to interpret with a previous publication reporting a difference in enthalpy between the two polymorphs in the order of 0 J g^{-1}. In the present paper, the observation of a direct transformation of form I into form II without an intermediate liquid phase made it possible to conclude that the enthalpy change is negative for the I $\rightarrow$ II transformation. Another difficulty is the wide range of observed glass transition temperatures, which still lacks a clear explanation.

Despite of the difficulties in obtaining reliable data, the topological phase diagram as represented in Figure 6 has been confirmed in two ways. Firstly, the obtention of the negative enthalpy difference for the transformation of form I into form II and the specific volume data of the two solid forms have led unequivocally to the schematic phase diagram in Figure 5. Secondly, the calculations using the Clapeyron equation demonstrating the intersection of the two solid – liquid equilibria at high pressure and temperature confirm the topological result obtained through the Le Chatelier principle. Unfortunately, the experimental data on the melting equilibrium of form I and the metastable I-II transition is not precise enough to accurately define the I-II-L triple point, which remains an estimate. Subsequently, the I-II equation, which depends on the location of the I-II-L triple point, can only be tentatively described, even if it is clear that its slope is negative.

An exothermic transformation of one solid form into another has previously been observed for biclotymol, however in that case the two melting equilibria diverge and only a single stable polymorph exists: overall monotropy (Ceolin et al., 2008). The phase diagram of spironolactone is surprisingly similar to that of paracetamol, with one form metastable under ordinary conditions, but stable under pressure (Barrio et al., 2017b; Espeau et al., 2005; Ledru et al., 2007). Furthermore, the solid-solid equilibrium line is also negative for paracetamol (Barrio et al., 2017b; Espeau et al., 2005; Ledru et al., 2007). In more general terms, the phase diagram of spironolactone belongs to the third case among the four possible cases of dimorphism described by Bakhuis-Roozeboom (Bakhuis Roozeboom, 1901).

The experimental difficulties notwithstanding, spironolactone is interesting due to the extremely rare difference of seventy degrees between the melting points of its two polymorphs as can be concluded from the data compiled by Burger and Ramberger (Burger and Ramberger, 1979b) and from more recently obtained data (Table 1). It is unexpected that the lower melting polymorph actually possesses a stable domain in the pressure-temperature phase diagram, because it goes against the rule of thumb that the densest form is also the most stable. Taking into consideration the shallowness of the slopes of the two melting equilibria and the fact that they are very similar, one must conclude that the Gibbs free energy surfaces of the two polymorphs are most likely rather close to each other despite the large difference in melting points. The closeness in Gibbs free energy can also be inferred from the observation that form I shows little tendency to transform into form II and thus that a strong driving force for this transition is lacking. This is validated by the fact that both polymorphs do not contain hydrogen bonds and thus that the main interactions involve only Van der Waals forces and thus no strong energy barriers are expected that restrict phase transformations.

CONFLICT OF INTEREST

The authors declare no conflict of interest

ACKNOWLEDGMENTS

This work was supported by the Spanish Ministry of Science and Innovation [grant number FIS2017-82625-P] and by the Generalitat de Catalunya [grant number 2017 SGR-0042].

REFERENCES

Agafonov, V., Legendre, B., Rodier, N., 1989. A New Crystalline Modification of Spironolactone. Acta Crystallogr. C 45, 1661-1663.
Agafonov, V., Legendre, B., Rodier, N., 1991a. Crystal Structure of the Solvate Spironolactone-Acetonitrile (2-1). Acta Crystallogr. C 47, 365-369.
Agafonov, V., Legendre, B., Rodier, N., Wouessidjewe, D., Cense, J.M., 1991b. Polymorphism of Spironolactone. J. Pharm. Sci. 80, 181-185.
Aitipamula, S., Chow, P.S., Tan, R.B.H., 2011. Conformational Polymorphs of a Muscle Relaxant, Metaxalone. Cryst. Growth Des. 11, 4101-4109.
Bakhuis Roozeboom, H.W., 1901. Die heterogenen Gleichgewichte vom Standpunkte der Phasenlehre. Erstes Heft: Die Phasenlehre - Systeme aus einer Komponente. Friedrich Vieweg und Sohn, Braunschweig.
Barrio, M., Huguet, J., Rietveld, I.B., Robert, B., Ceolin, R., Tamarit, J.L., 2017a. The Pressure-Temperature Phase Diagram of Metacetamol and Its Comparison to the Phase Diagram of Paracetamol. J. Pharm. Sci. 106, 1538-1544.
Barrio, M., Huguet, J., Rietveld, I.B., Robert, B., Ceolin, R., Tamarit, J.L., 2017b. The pressure-temperature phase diagram of metacetamol and its comparison to the phase diagram of paracetamol. J. Pharm. Sci. 106, 1538-1544.
Barrio, M., Huguet, J., Robert, B., Rietveld, I.B., Ceolin, R., Tamarit, J.L., 2017c. Pressure-temperature phase diagram of the dimorphism of the anti-inflammatory drug nimesulide. Int. J. Pharm. 525, 54-59.
Barrio, M., Tamarit, J.L., Ceolin, R., Robert, B., Guechot, C., Teulon, J.M., Rietveld, I.B., 2017d. Experimental and topological determination of the pressure temperature phase diagram of morniflumate, a pharmaceutical ingredient with anti-inflammatory properties. J. Chem. Thermodyn. 112, 308-313.
Barsky, I., Bernstein, J., Stephens, P.W., Stone, K.H., Cheung, E., Hickey, M.B., Henck, J.O., 2008. Disappearing and reappearing polymorphism in p-methylchalcone. Cryst. Growth Des. 8, 63-70.
Bartolomei, M., Bertocchi, P., Ramusino, M.C., Signoretti, E.C., 1998. Thermal studies on the polymorphic modifications of (R,S) propranolol hydrochloride. Thermochim. Acta 321, 43-52.
Bauer, J., Morley, J., Spanton, S., Leusen, F.J.J., Henry, R., Hollis, S., Heitmann, W., Mannino, A., Quick, J., Dziki, W., 2006. Identification, preparation, and characterization of several polymorphs and solvates of terazosin hydrochloride. J. Pharm. Sci. 95, 917-928.
Berbenni, V., Marini, A., Bruni, G., Maggioni, A., Riccardi, R., Orlandi, A., 1999. Physico-chemical characterisation of different solid forms of spironolactone. Thermochim. Acta 341, 117-129.
Bohlin, M.S., SE), Cosgrove, Steve (Loughborough, GB), Lassen, Bo (Södertälje, SE),, 2007. Cristalline and amorphous form of a triazolo (4,5-D) pyridimine compound. AstraZeneca AB (Sodertalje, SE), United States.
Bolla, G., Mittapalli, S., Nangia, A., 2014. Pentamorphs of Acedapsone. Cryst. Growth Des. 14, 5260-5274.
Bottom, R., 1999. The role of modulated temperature differential scanning calorimetry in the characterisation of a drug molecule exhibiting polymorphic and glass forming tendencies. Int. J. Pharm. 192, 47-53.
Braga, D., Grepioni, F., Chelazzi, L., Nanna, S., Rubini, K., Curzi, M., Giaffreda, S.L., Saxell, H.E., Bratz, M., Chiodo, T., 2014. Bentazon: Effect of Additives on the Crystallization of Pure and Mixed Polymorphic Forms of a Commercial Herbicide. Cryst. Growth Des. 14, 5729-5736.
Brandão, F.C., Tagiari, M.P., Silva, M.A.S., Berti, L.F., Stulzer, H.K., 2008. Physical-chemical characterization and quality control of spironolactone raw material samples. Pharm. Chem. J. 42, 368-376.
Braun, D.E., Gelbrich, T., Jetti, R.K.R., Kahlenberg, V., Price, S.L., Griesser, U.J., 2008a. Colored polymorphs: Thermochemical and structural features of N-picryl-p-toluidine polymorphs and solvates. Cryst. Growth Des. 8, 1977-1989.
Braun, D.E., Gelbrich, T., Kahlenberg, V., Laus, G., Wieser, J., Griesser, U.J., 2008b. Packing polymorphism of a conformationally flexible molecule (aprepitant). New J. Chem. 32, 1677-1685.
Braun, D.E., Gelbrich, T., Kahlenberg, V., Tessadri, R., Wieser, J., Griesser, U.J., 2009. Conformational Polymorphism in Aripiprazole: Preparation, Stability and Structure of Five Modifications. J. Pharm. Sci. 98, 2010-2026.
Bruni, G., Berbenni, V., Milanese, C., Girella, A., Cardini, A., Vigano, E., Lanfranconi, S., Marini, A., 2009. Thermodynamic relationships between nateglinide polymorphs. J. Pharm. Biomed. Anal. 50, 764-770.
Bruni, G., Pardi, F., Capsoni, D., Berbenni, V., Bini, M., Valle, G., Milanese, C., Girella, A., Marini, A., 2017. Febantel: looking for new polymorphs. J. Therm. Anal. Calorim. 130, 1605-1612.

Burger, A., Lettenbichler, A., 2000. Polymorphism and preformulation studies of lifibrol. Eur. J. Pharm. Biopharm. 49, 65-72.
Burger, A., Ramberger, R., 1979a. Polymorphism of Pharmaceuticals and Other Molecular-Crystals .1. Theory of Thermodynamic Rules. Mikrochim. Acta 2, 259-271.
Burger, A., Ramberger, R., 1979b. Polymorphism of Pharmaceuticals and Other Molecular-Crystals .2. Applicability of Thermodynamic Rules. Mikrochim. Acta 2, 273-316.
Burger, A., Rollinger, J.M., Bruggeller, P., 1997. Binary system of (R)- and (S)-nitrendipine - Polymorphism and structure. J. Pharm. Sci. 86, 674-679.
Caira, M.R., Bourne, S.A., Oliver, C.L., 2004a. Thermal and structural characterization of two polymorphs of the bronchodilator tulobuterol. J. Therm. Anal. Calorim. 77, 597-605.
Caira, M.R., Foppoli, A., Sangalli, M.E., Zema, L., Giordano, F., 2004b. Thermal and structural properties of ambroxol polymorphs. J. Therm. Anal. Calorim. 77, 653-662.
Carpentier, L., Rharrassi, K.F., Derollez, P., Guinet, Y., 2013. Crystallization and polymorphism of L-arabitol. Thermochim. Acta 556, 63-67.
Carrer, H., Cortez, J., Frare, L.M., Costa, M.B., Bittencourt, P.R.S., 2016. Thermal characterization of the bromopride recrystallized from different solvents and at different temperature conditions. J. Therm. Anal. Calorim. 123, 927-931.
Carvalho Jr, P.S., Ellena, J., Yufit, D.S., Howard, J.A., 2016. Rare case of polymorphism in a racemic Fluoxetine Nitrate salt: Phase Behavior and Relative Stability. Cryst. Growth Des.
Céolin, R., Agafonov, V., Louër, D., Dzyabchenko, V.A., Toscani, S., Cense, J.M., 1996. Phenomenology of Polymorphism, III:p,TDiagram and Stability of Piracetam Polymorphs. J. Solid State Chem. 122, 186-194.
Ceolin, R., Rietveld, I.B., 2017. Thermodynamic origin and graphical methods of phase theory. Eur. Phys. J. - S.T. 226, 1001-1015.
Céolin, R., Rietveld, I.B., 2015. The topological pressure-temperature phase diagram of ritonavir, an extraordinary case of crystalline dimorphism. Ann. Pharm. Fr. 73, 22-30.
Ceolin, R., Tamarit, J.L., Barrio, M., Lopez, D.O., Nicolai, B., Veglio, N., Perrin, M.A., Espeau, P., 2008. Overall monotropic behavior of a metastable phase of biclotymol, 2,2'-methylenebis(4-chloro-3-methyl-isopropylphenol), inferred from experimental and topological construction of the related P-T state diagram. J. Pharm. Sci. 97, 3927-3941.
Chemburkar, S.R., Bauer, J., Deming, K., Spiwek, H., Patel, K., Morris, J., Henry, R., Spanton, S., Dziki, W., Porter, W., Quick, J., Bauer, P., Donaubauer, J., Narayanan, B.A., Soldani, M., Riley, D., McFarland, K., 2000. Dealing with the impact of ritonavir polymorphs on the late stages of bulk drug process development. Org Process Res Dev 4, 413-417.
Chikaraishi, Y., Sano, A., Tsujiyama, T., Otsuka, M., Matsuda, Y., 1994. Preparation of Piretanide Polymorphs and Their Physicochemical Properties and Dissolution Behaviors. Chem Pharm Bull 42, 1123-1128.
De Armas, H.N., Peeters, O.M., Blaton, N., Van den Mooter, G., De Ridder, D.J.A., Schenk, H., 2006. Crystal structure of carnidazole form II from synchrotron X-ray powder diffraction: Structural comparison with form I, the hydrated form and the low energy conformations in vacuo. J. Pharm. Sci. 95, 2123-2136.
De Armas, H.N., Peeters, O.M., Blaton, N., Van Gyseghem, E., Martens, J., Van Haele, G., Van den Mooter, G., 2009. Solid State Characterization and Crystal Structure from X-Ray Powder Diffraction of Two Polymorphic Forms of Ranitidine Base. J. Pharm. Sci. 98, 146-158.
De Armas, H.N., Peeters, O.M., Van den Mooter, G., Blaton, N., 2007. Polymorphism of Alprazolam (Xanax (R)): A review of its crystalline phases and identification, crystallographic characterization, and crystal structure of a new polymorph (Form III). J. Pharm. Sci. 96, 1114-1130.
De Resende, R.C., Viana, O.M.M.S., Freitas, J.T.J., Bonfilio, R., Ruela, A.L.M., De Araujo, M.B., 2016. Analysis of spironolactone polymorphs in active pharmaceutical ingredients and their effect on tablet dissolution profiles. Braz J Pharm Sci 52, 613-621.
Detrich, Á., Dömötör, K.J., Katona, M.T., Markovits, I., Vargáné Láng, J., 2018. Polymorphic forms of bisoprolol fumarate. J. Therm. Anal. Calorim. in press.
Dideberg, O., Dupont, L., 1972. Crystal and Molecular Structure of Spironolactone (7alpha-Acetylthio-3-Oxo-17alpha-4-Pregnene-21, 17beta-Carbolactone). Acta Crystallogr. B 28, 3014-3022.
Dinnebier, R.E., Sieger, P., Nar, H., Shankland, K., David, W.I.F., 2000. Structural characterization of three crystalline modifications of telmisartan by single crystal and high-resolution X-ray powder diffraction. J. Pharm. Sci. 89, 1465-1479.
Dong, Y.C., Ng, W.K., Shen, S.C., Kim, S., Tan, R.B.H., 2009. Preparation and characterization of spironolactone nanoparticles by antisolvent precipitation. Int. J. Pharm. 375, 84-88.
Dong, Z.D., Munson, E.J., Schroeder, S.A., Prakash, I., Grant, D.J.W., 2002. Neotame anhydrate polymorphs II: Quantitation and relative physical stability. Pharm. Res. 19, 1259-1264.
Eldalsh, S.S., Elsayed, A.A., Badawi, A.A., Khattab, F.I., Fouli, A., 1983. Studies on Spironolactone Polymorphic Forms. Drug Dev. Ind. Pharm. 9, 877-894.

Espeau, P., Céolin, R., Tamarit, J.L., Perrin, M.A., Gauchi, J.P., Leveiller, F., 2005. Polymorphism of paracetamol: Relative stabilities of the monoclinic and orthorhombic phases inferred from topological pressure-temperature and temperature-volume phase diagrams. J. Pharm. Sci. 94, 524-539.
Espeau, P., Nicolai, B., Ceolin, R., Perrin, M.A., Zaske, L., Giovannini, J., Leveiller, F., 2007. Thermal behavior of orthorhombic polymorphs I and II of spironolactone. J. Therm. Anal. Calorim. 90, 341-342.
Florence, A.T., Salole, E.G., 1976. Changes in Crystallinity and Solubility on Comminution of Digoxin and Observations on Spironolactone and Estradiol. J. Pharm. Pharmacol. 28, 637-642.
Foppoli, A., Sangalli, M.E., Maroni, A., Gazzaniga, A., Caira, M.R., Giordano, F., 2004. Polymorphism of NCX4016, an NO-releasing derivative of acetylsalicylic acid. J. Pharm. Sci. 93, 521-531.
Fukuoka, E., Makita, M., Nakamura, Y., 1991. Glassy State of Pharmaceuticals .5. Relaxation during Cooling and Heating of Glass by Differential Scanning Calorimetry. Chem Pharm Bull 39, 2087-2090.
Gana, I., Céolin, R., Rietveld, I.B., 2013. Bicalutamide polymorphs I and II. J. Therm. Anal. Calorim. 112, 223-228.
Gavezzotti, A., 2013. Molecular Aggregation. Structure Analysis and Molecular Simulation of Crystals and Liquids. Oxford University Press, Oxford, UK.
Gelbrich, T., Braun, D.E., Ellern, A., Griesser, U.J., 2013. Four Polymorphs of Methyl Paraben: Structural Relationships and Relative Energy Differences. Cryst. Growth Des. 13, 1206-1217.
Ghodbane, S., Mccauley, J.A., 1990. Study of the Polymorphism of 3-(((3-(2-(7-Chloro-2-Quinolinyl)(E)-Ethenyl)Phenyl)((3-(Dimethylamino-3-Oxopropyl)Thio)Methyl)Thio)Propanoic Acid (Mk571) by Dsc, Tg, Xrpd and Solubility Measurements. Int. J. Pharm. 59, 281-286.
Giordano, F., Gazzaniga, A., Moyano, J.R., Ventura, P., Zanol, M., Peveri, T., Carima, L., 1998. Crystal forms of piroxicam pivalate: Preparation and characterization of two polymorphs. J. Pharm. Sci. 87, 333-337.
Giovannini, J., Ter Minassian, L., Ceolin, R., Toscani, S., Perrin, M.A., Louer, D., Leveiller, F., 2001. Tetramorphism of fananserine: p, T diagram and stability hierarchy from crystal structure determinations and thermodynamic studies. J. Phys. IV 11, 123-126.
Gong, N.B., Zhang, G.S., Jin, G.M., Du, G.H., Lu, Y., 2016. Polymorphs and Versatile Solvates of 7-Hydroxyisoflavone. J. Pharm. Sci. 105, 1387-1397.
Goodman, B.T., Wilding, W.V., Oscarson, J.L., Rowley, R.L., 2004. A note on the relationship between organic solid density and liquid density at the triple point. J. Chem. Eng. Data 49, 1512-1514.
Grcman, M., Vrecer, F., Meden, A., 2002. Some physico-chemical properties of doxazosin mesylate polymorphic forms and its amorphous state. J. Therm. Anal. Calorim. 68, 373-387.
Griesser, U.J., Weigand, D., Rollinger, J.M., Haddow, M., Gstrein, E., 2004. The crystal polymorphs of metazachlor - Identification and thermodynamic stability. J. Therm. Anal. Calorim. 77, 511-522.
Grillo, D., Polla, G., Vega, D., 2012. Conformational polymorphism on imatinib mesylate: Grinding effects. J. Pharm. Sci. 101, 541-551.
Gu, X.J., Jiang, W., 1995. Characterization of Polymorphic Forms of Fluconazole Using Fourier-Transform Raman-Spectroscopy. J. Pharm. Sci. 84, 1438-1441.
Guo, J., Ulrich, J., 2010. Polymorphism and solvates of 3,3 '-dihydroxy-beta,beta-carotene-4,4 '-dione: Screening and their thermodynamics. Cryst. Res. Technol. 45, 267-274.
He, F., Wang, Y.L., Yin, Q.X., Tao, L.G., Lv, J., Xu, Z., Wang, J.X., Hao, H.X., 2016. Effect of polymorphism on thermodynamic properties of cefamandole nafate. Fluid Phase Equilib. 422, 56-65.
Henck, J.O., Kuhnert-Brandstatter, M., 1999. Demonstration of the terms enantiotropy and monotropy in polymorphism research exemplified by flurbiprofen. J. Pharm. Sci. 88, 103-108.
Herman, C., Leyssens, T., Vermylen, V., Halloin, V., Haut, B., 2011. Towards an accurate and precise determination of the solid-solid transition temperature of enantiotropic systems. J. Chem. Thermodyn. 43, 677-682.
Jarring, K., Larsson, T., Stensland, B., Ymen, I., 2006. Thermodynamic stability and crystal structures for polymorphs and solvates of formoterol fumarate. J. Pharm. Sci. 95, 1144-1161.
Jetti, R.K.R., Bhogala, B.R., Gorantla, A.R., Karusula, N.R., Datta, D., 2011. Structural and Thermodynamic Features of Three Stable Crystal Forms of Temazepam: A Sedative Drug. Cryst. Growth Des. 11, 2039-2044.
Jiang, C., Yan, J.Q., Wang, Y.L., Zhang, J., Wang, G., Yang, J.X., Hao, H.X., 2015. Isolation Strategies and Transformation Behaviors of Spironolactone Forms. Ind Eng Chem Res 54, 11222-11229.
Joseph, A., Bernardes, C.E.S., Druzhinina, A.I., Varushchenko, R.M., Nguyen, T.Y., Emmerling, F., Yuan, L.N., Dupray, V., Coquerel, G., da Piedade, M.E.M., 2017. Polymorphic Phase Transition in 4 '-Hydroxyacetophenone: Equilibrium Temperature, Kinetic Barrier, and the Relative Stability of Z '=1 and Z '=2 Forms. Cryst. Growth Des. 17, 1918-1932.
Jozwiakowski, M.J., Nguyen, N.T., Sisco, J.M., Spancake, C.W., 1996. Solubility behavior of lamivudine crystal forms in recrystallization solvents. J. Pharm. Sci. 85, 193-199.

Jurcek, O., Lahtinen, M., Wimmer, Z., Drasar, P., Kolehmainen, E., 2012. Crystallization, Spectral, Crystallographical, and Thermoanalytical Studies of Succinobucol Polymorphism. J. Pharm. Sci. 101, 1794-1802.
Kawakami, K., Ohba, C., 2017. Crystallization of probucol from solution and the glassy state. Int. J. Pharm. 517, 322-328.
Khomane, K.S., More, P.K., Bansal, A.K., 2012. Counterintuitive Compaction Behavior of Clopidogrel Bisulfate Polymorphs. J. Pharm. Sci. 101, 2408-2416.
Kushida, I., Ashizawa, K., 2002. Solid state characterization of E2101, a novel antispastic drug. J. Pharm. Sci. 91, 2193-2202.
Laine, E., Pirttimaki, J., Rajala, R., 1995. Thermal Studies on Polymorphic Structures of Ibopamin. Thermochim. Acta 248, 205-216.
Lara-Ochoa, F., Perez, G.E., Mijangos-Santiago, F., 2007. Calorimetric determinations and theoretical calculations of polymorphs of thalidomide. J. Mol. Struct. 840, 97-106.
Laszcz, M., Trzcinska, K., Witkowska, A., Ciesielska, A., Badowska-Roslonek, K., Kuziak, K., 2016. Structural and Physicochemical Studies of Olopatadine Hydrochloride Conformational Polymorphs. J. Pharm. Sci. 105, 2419-2426.
Latosinska, J.N., Latosinska, M., Szafranski, M., Seliger, J., Zagar, V., 2016. Polymorphism and Thermal Stability of Natural Active Ingredients. 3,3 '-Diindolylmethane (Chemopreventive and Chemotherapeutic) Studied by a Combined X-ray, H-1-N-14 NMR-NQR, Differential Scanning Calorimetry, and Solid-State DFT/3D HS/QTAIM/RDS Computational Approach. Cryst. Growth Des. 16, 4336-4348.
Ledru, J., Imrie, C.T., Pulham, C.R., Céolin, R., Hutchinson, J.M., 2007. High pressure differential scanning Calorimetry investigations on the pressure dependence of the melting of paracetamol polymorphs I and II. J. Pharm. Sci. 96, 2784-2794.
Leitao, M.L.P., Canotilho, J., Cruz, M.S.C., Pereira, J.C., Sousa, A.T., Redinha, J.S., 2002. Study of polymorphism from DSC melting curves - Polymorphs of terfenadine. J. Therm. Anal. Calorim. 68, 397-412.
Liebenberg, W., van Tonder, E.C., Dekker, T.G., de Villiers, M.M., 2003. Variable temperature X-ray powder diffractometry of spironolactone polymorphs. Pharmazie 58, 435-437.
Lindenbaum, S., Rattie, E.S., Zuber, G.E., Miller, M.E., Ravin, L.J., 1985. Polymorphism of Auranofin. Int. J. Pharm. 26, 123-132.
Lu, G.W., Hawley, M., Smith, M., Geiger, B.M., Pfund, W., 2006. Characterization of a novel polymorphic form of celecoxib. J. Pharm. Sci. 95, 305-317.
Lu, J., Rohani, S., 2009. Polymorphic Crystallization and Transformation of the Anti-Viral/HIV Drug Stavudine. Org Process Res Dev 13, 1262-1268.
Lu, J., Wang, X.J., Yang, X., Ching, C.B., 2007. Polymorphism and crystallization of Famotidine. Cryst. Growth Des. 7, 1590-1598.
Maccaroni, E., Alberti, E., Malpezzi, L., Masciocchi, N., Vladiskovic, C., 2008. Polymorphism of linezolid: A combined single-crystal, powder diffraction and NMR study. Int. J. Pharm. 351, 144-151.
Maccaroni, E., Malpezzi, L., Panzeri, W., Masciocchi, N., 2010. Thermal and X-ray powder diffraction structural characterization of two benfluorex hydrochloride polymorphs. J Pharm Biomed Anal 53, 1-6.
Mahé, N., Perrin, M., Barrio, M., Nicolaï, B., Rietveld, I., Tamarit, J., Céolin, R., 2011. Solid-State Studies of the Triclinic (Z '=2) Antiprotozoal Drug Ternidazole. J. Pharm. Sci. 100, 2258-2266.
Mahlin, D., Bergstrom, C.A.S., 2013. Early drug development predictions of glass-forming ability and physical stability of drugs. Eur J Pharm Sci 49, 323-332.
Malaj, L., Censi, R., Capsoni, D., Pellegrino, L., Bini, M., Ferrari, S., Gobetto, R., Massarotti, V., Di Martino, P., 2011. Characterization of Nicergoline Polymorphs Crystallized in Several Organic Solvents. J. Pharm. Sci. 100, 2610-2622.
Maria, T.M.R., Castro, R.A.E., Ramos Silva, M.R., Ramos, M.L., Justino, L.L.G., Burrows, H.D., Canotilho, J., Eusebio, M.E.S., 2013. Polymorphism and melt crystallisation of racemic betaxolol, a beta-adrenergic antagonist drug. J. Therm. Anal. Calorim. 111, 2171-2178.
Marini, A., Berbenni, V., Bruni, G., Maggioni, A., Orlandi, A., Villa, M., 2001. Thermodynamics of a complex melting process: the case of spironolactone. Thermochim. Acta 374, 171-184.
McGregor, L., Rychkov, D.A., Coster, P.L., Day, S., Drebushchak, V.A., Achkasov, A.F., Nichol, G.S., Pulham, C.R., Boldyreva, E.V., 2015. A new polymorph of metacetamol. CrystEngComm 17, 6183-6192.
Mesley, R.J., Johnson, C.A., 1965. Infrared Identification of Pharmaceutically Important Steroids with Particular Reference to Occurrence of Polymorphism. J. Pharm. Pharmacol. 17, 329-&.
Michalak, O., Laszcz, M., Jatczak, K., Witkowska, A., Bujak, I., Groman, A., Cybulski, M., 2015. New Polymorphic Forms of Pemetrexed Diacid and Their Use for the Preparation of Pharmaceutically Pure Amorphous and Hemipentahydrate Forms of Pemetrexed Disodium. Molecules 20, 13814-13829.
Mirmehrabi, M., Rohani, S., Murthy, K.S.K., Radatus, B., 2004. Characterization of tautomeric forms of ranitidine hydrochloride: thermal analysis, solid-state NMR, X-ray. J. Cryst. Growth 260, 517-526.

Mitchell, A.G., 1985. Polymorphism in Metoclopramide Hydrochloride and Metoclopramide. J. Pharm. Pharmacol. 37, 601-604.
Miyamae, A., Kitamura, S., Tada, T., Koda, S., Yasuda, T., 1991. X-Ray Structural Studies and Physicochemical Characterization of (E)-6-(3,4-Dimethoxyphenyl)-1-Ethyl-4-Mesitylimino-3-Methyl-3,4-Dihydro-2(1h)-Pyrimidinone Polymorphs. J. Pharm. Sci. 80, 995-1000.
Moreno-Calvo, E., Munto, M., Wurst, K., Ventosa, N., Masciocchi, N., Veciana, J., 2011. Polymorphs and Solvates of Nicardipine Hydrochloride. Selective Stabilization of Different Diastereomeric Racemates. Mol. Pharmaceut. 8, 395-404.
Murphy, B.J., Huang, J., Casteel, M.J., Cobani, A., Krzyzaniak, J.F., 2010. Varenicline L-tartrate Crystal Forms: Characterization Through Crystallography, Spectroscopy, and Thermodynamics. J. Pharm. Sci. 99, 2766-2776.
Nagai, K., Ushio, T., Miura, H., Nakamura, T., Moribe, K., Yamamoto, K., 2014. Four new polymorphic forms of suplatast tosilate. Int. J. Pharm. 460, 83-91.
Nicolai, B., Espeau, P., Ceolin, R., Perrin, M.A., Zaske, L., Giovannini, J., Leveiller, F., 2007. Polymorph formation from solvate desolvation spironolactone forms I and II from the spironolactone-ethanol solvate. J. Therm. Anal. Calorim. 90, 337-339.
Oguchi, T., Sasaki, N., Hara, T., Tozuka, Y., Yamamoto, K., 2003. Differentiated thermal crystallization from amorphous chenodeoxycholic acid between the ground specimens derived from the polymorphs. Int. J. Pharm. 253, 81-88.
Park, Y., Lee, J., Lee, S.H., Choi, H.G., Mao, C., Kang, S.K., Choi, S.E., Lee, E.H., 2013. Crystal Structures of Tetramorphic Forms of Donepezil and Energy/Temperature Phase Diagram via Direct Heat Capacity Measurements. Cryst. Growth Des. 13, 5450-5458.
Patel, J., Jagia, M., Bansal, A.K., Patel, S., 2015. Characterization and Thermodynamic Relationship of Three Polymorphs of a Xanthine Oxidase Inhibitor, Febuxostat. J. Pharm. Sci. 104, 3722-3730.
Pereira-Silva, P.S., Castro, R.A.E., Melro, E., Ramos-Silva, M., Maria, T.M.R., Canotilho, J., Eusebio, M.E.S., 2015. Structural evidence of polymorphism and conformational isomorphism of a somewhat flexible molecule: m-anisic acid. J. Therm. Anal. Calorim. 120, 667-677.
Perlovich, G.L., Hansen, L.K., Bauer-Brandl, A., 2002. Interrelation between thermochemical and structural data of polymorphs exemplified by diflunisal. J. Pharm. Sci. 91, 1036-1045.
Perrin, M.A., Bauer, M., Barrio, M., Tamarit, J.L., Ceolin, R., Rietveld, I.B., 2013. Rimonabant dimorphism and its pressure-temperature phase diagram: a delicate case of overall monotropic behavior. J. Pharm. Sci. 102, 2311-2321.
Pfeiffer, I.W., NC, US), Whittle, Robert R. (Wilmington, NC, US), Stowell, Grayson Walker (Wilmington, NC, US), Whittall, Linda B. (Wilmington, NC, US), 2003. Polymorphic form of 3-[2-[4-(6-fluoro-1,2-benzisoxazol-3-yl)-1-piperidinyl]ethyl]-6,7,8,9-tetrahydro-2-methyl-4h-pyrido[1,2-alpha]pyrimidin-4-one and formulations thereof. PFEIFFER INIGO,WHITTLE ROBERT R.,STOWELL GRAYSON WALKER,WHITTALL LINDA B., United States.
Pfund, L.Y., Chamberlin, B.L., Matzger, A.J., 2015. The Bioenhancer Piperine is at Least Trimorphic. Cryst. Growth Des. 15, 2047-2051.
Pisegna, G.L., 1999. A High-pressure Vibrational spectroscopic study of polymorphism in steroids: progesterone and spironolactone. McGill University, Montreal.
Pranzo, M.B., Cruickshank, D., Coruzzi, M., Caira, M.R., Bettini, R., 2010. Enantiotropically Related Albendazole Polymorphs. J. Pharm. Sci. 99, 3731-3742.
Price, C.P., Grzesiak, A.L., Lang, M., Matzger, A.J., 2002. Polymorphism of nabumetone. Cryst. Growth Des. 2, 501-503.
Qi, M.H., Hong, M.H., Liu, Y., Wang, E.F., Ren, F.Z., Ren, G.B., 2015. Estimating Thermodynamic Stability Relationship of Polymorphs of Sofosbuvir. Cryst. Growth Des. 15, 5062-5067.
Rafilovich, M., Bernstein, J., 2006. Serendipity and four polymorphic structures of benzidine, C12H12N2. J. Am. Chem. Soc. 128, 12185-12191.
Raghavan, K., Dwivedi, A., Campbell, G.C., Nemeth, G., Hussain, M.A., 1994. A Spectroscopic Investigation of Dup-747 Polymorphs. J. Pharm. Biomed. Anal. 12, 777-785.
Reepmeyer, J.C., Rhodes, M.O., Cox, D.C., Silverton, J.V., 1994. Characterization and Crystal-Structure of 2 Polymorphic Forms of Racemic Thalidomide. J Chem Soc Perk T 2, 2063-2067.
Reutzel-Edens, S.M., Kleemann, R.L., Lewellen, P.L., Borghese, A.L., Antoine, L.J., 2003. Crystal forms of LY334370 HCl: Isolation, solid-state characterization, and physicochemical properties. J. Pharm. Sci. 92, 1196-1205.
Rietveld, I.B., Ceolin, R., 2015. Rotigotine: Unexpected Polymorphism with Predictable Overall Monotropic Behavior. J. Pharm. Sci. 104, 4117-4122.
Rietveld, I.B., Céolin, R., 2015. Phenomenology of crystalline polymorphism: overal monotropic behavior of the cardiotonic agent FK664 forms A and B. J. Therm. Anal. Calorim. 120, 1079-1087.

Rietveld, I.B., Perrin, M.-A., Toscani, S., Barrio, M., Nicolaï, B., Tamarit, J.-L., Céolin, R., 2013. Liquid-Liquid Miscibility Gaps in Drug-Water Binary Systems: Crystal Structure and Thermodynamic Properties of Prilocaine and the Temperature-Composition Phase Diagram of the Prilocaine-Water System. Mol. Pharmaceut. 10, 1332-1339.
Robert, B., Perrin, M.A., Barrio, M., Tamarit, J.L., Coquerel, G., Ceolin, R., Rietveld, I.B., 2016. Crystal Structures and Phase Relationships of 2 Polymorphs of 1,4-Diazabicyclo[3.2.2]nonane-4-Carboxylic Acid 4-Bromophenyl Ester Fumarate, A Selective alpha-7 Nicotinic Receptor Partial Agonist. J. Pharm. Sci. 105, 64-70.
Rocco, W.L., Swanson, J.R., 1995. Win-63843 Polymorphs - Prediction of Enantiotropy. Int. J. Pharm. 117, 231-236.
Rossi, D., Gelbrich, T., Kahlenberg, V., Griesser, U.J., 2012. Supramolecular constructs and thermodynamic stability of four polymorphs and a co-crystal of pentobarbital (nembutal). CrystEngComm 14, 2494-2506.
Roy, S., Aitipamula, S., Nangia, A., 2005. Thermochemical analysis of venlafaxine hydrochloride polymorphs 1-5. Cryst. Growth Des. 5, 2268-2276.
Roy, S., Bhatt, P.M., Nangia, A., Kruger, G.J., 2007. Stable polymorph of venlafaxine hydrochloride by solid-to-solid phase transition at high temperature. Cryst. Growth Des. 7, 476-480.
Saito, M., Matsumura, K., Kato, H., Ito, Y., 1983. Polymorphism of Alpha-[(Tert-Butylamino)Methyl]-2-Chloro-4-Hydroxybenzyl Alcohol Hydrochloride (Hoku-81). Chem Pharm Bull 31, 1101-1104.
Saito, M., Yabu, H., Yamazaki, M., Matsumura, K., Kato, H., 1982. Studies on the Relationship between Physicochemical Properties and Crystalline Forms of Tulobuterol Hydrochloride .1. Polymorphism of Tulobuterol Hydrochloride. Chem Pharm Bull 30, 652-658.
Salole, E.G., Alsarraj, F.A., 1985a. Effect of Solvent-Deposition on Spironolactone Crystal Form. Drug Dev. Ind. Pharm. 11, 2061-2070.
Salole, E.G., Alsarraj, F.A., 1985b. Spironolactone Crystal Forms. Drug Dev. Ind. Pharm. 11, 855-864.
Sanphui, P., Goud, N.R., Khandavilli, U.B.R., Bhanoth, S., Nangia, A., 2011. New polymorphs of curcumin. Chem. Commun. 47, 5013-5015.
Saunier, J., Mazel, V., Aymes-Chodur, C., Yagoubi, N., 2012. Blooming of Irganox 3114 (R) antioxidant onto a medical grade elastomer. Impact of the recrystallization conditions on the antioxidant polymorphism, on the film wettability and on the antioxidant leachability. Int. J. Pharm. 437, 89-99.
Saunier, J., Mazel, V., Paris, C., Yagoubi, N., 2010. Polymorphism of Irganox 1076 (R): Discovery of new forms and direct characterization of the polymorphs on a medical device by Raman microspectroscopy. Eur. J. Pharm. Biopharm. 75, 443-450.
Schinzer, W.C., Bergren, M.S., Aldrich, D.S., Chao, R.S., Dunn, M.J., Jeganathan, A., Madden, L.M., 1997. Characterization and interconversion of polymorphs of premafloxacin, a new quinolone antibiotic. J. Pharm. Sci. 86, 1426-1431.
Schmidt, A.C., Niederwanger, V., Griesser, U.J., 2004. Solid-state forms of prilocaine hydrochloride - Crystal polymorphism of local anaesthetic drugs, Part II. J. Therm. Anal. Calorim. 77, 639-652.
Schmidt, A.C., Schwarz, I., Mereiter, K., 2006. Polymorphism and pseudopolymorphism of salicaine and salicaine hydrochloride crystal polymorphism of local anaesthetic drugs, part V. J. Pharm. Sci. 95, 1097-1113.
Sheikhzadeh, M., Rohani, S., Jutan, A., Manifar, T., Murthy, K., Horne, S., 2006. Solid-state characterization of buspirone hydrochloride polymorphs. Pharm. Res. 23, 1043-1050.
Shibata, M., Kokubo, H., Morimoto, K., Morisaka, K., Ishida, T., Inoue, M., 1983. X-ray structural studies and physicochemical properties of cimetidine polymorphism. J. Pharm. Sci. 72, 1436-1442.
Singh, P., Chadha, R., 2017. A new polymorph of ciprofloxacin saccharinate: Structural characterization and pharmaceutical profile. J. Pharm. Biomed. Anal. 146, 7-14.
Snider, D.A., Addicks, W., Owens, W., 2004. Polymorphism in generic drug product development. Adv Drug Deliver Rev 56, 391-395.
Srcic, S., Kerc, J., Urleb, U., Zupancic, I., Lahajnar, G., Kofler, B., Smidkorbar, J., 1992. Investigation of Felodipine Polymorphism and Its Glassy State. Int. J. Pharm. 87, 1-10.
Stephenson, G.A., Liang, C., 2006. Structural determination of the stable and meta-stable forms of atomoxetine HCl using single crystal and powder X-ray diffraction methods. J. Pharm. Sci. 95, 1677-1683.
Stowell, G.W., Behme, R.J., Denton, S.M., Pfeiffer, I., Sancilio, F.D., Whittall, L.B., Whittle, R.R., 2002. Thermally-prepared polymorphic forms of cilostazol. J. Pharm. Sci. 91, 2481-2488.
Sun, Z.H., Hao, H.X., Xie, C., Xu, Z., Yin, Q.X., Bao, Y., Hou, B.H., Wang, Y.L., 2014. Thermodynamic Properties of Form A and Form B of Florfenicol. Ind Eng Chem Res 53, 13506-13512.
Sutter, J.L., Lau, E.P.K., 1975. Spironolactone, in: Florey, K. (Ed.), Analytical profile of drug substances. Academic Press, London, pp. 431-451.
Suzuki, E., Shimomura, K., Sekiguchi, K., 1989. Thermochemical Study of Theophylline and Its Hydrate. Chem Pharm Bull 37, 493-497.

Suzuki, T., Araki, T., Kitaoka, H., Terada, K., 2010. Studies on mechanism of thermal crystal transformation of sitafloxacin hydrates through melting and recrystallization, yielding different anhydrates depending on initial crystalline forms. Int. J. Pharm. 402, 110-116.
Svard, M., Nordstrom, F.L., Jasnobulka, T., Rasmuson, A.C., 2010. Thermodynamics and Nucleation Kinetics of in-Aminobenzoic Acid Polymorphs. Cryst. Growth Des. 10, 195-204.
Svard, M., Valavi, M., Khamar, D., Kuhs, M., Rasmuson, A.C., 2016. Thermodynamic Stability Analysis of Tolbutamide Polymorphs and Solubility in Organic Solvents. J. Pharm. Sci. 105, 1901-1906.
Takeguchi, K., Hirakura, Y., Yamazaki, K., Shimada, I., Ieda, S., Okada, M., Takiyama, H., 2015. Characterization and Thermodynamic Stability of Polymorphs of Di(arylamino) Aryl Compound ASP3026. Chem Pharm Bull 63, 418-422.
Thirunahari, S., Aitipamula, S., Chow, P.S., Tan, R.B., 2010. Conformational polymorphism of tolbutamide: A structural, spectroscopic, and thermodynamic characterization of Burger's forms I-IV. J. Pharm. Sci. 99, 2975-2990.
Todeschini, V., de Oliveira, P.R., Bernardi, L., Pereira, R.L., de Campos, C.E.M., Silva, M.A.S., Volpato, N.M., 2014. Delapril and manidipine characterization and purity evaluation in raw materials. J. Therm. Anal. Calorim. 115, 2295-2301.
Tong, H.H.Y., Shekunov, B.Y., York, P., Chow, A.H.L., 2001. Characterization of two polymorphs of salmeterol xinafoate crystallized from supercritical fluids. Pharm. Res. 18, 852-858.
Tros de Ilarduya, M.C., Martin, C., Goni, M.M., Martinez-Oharriz, M.C., 1997. Polymorphism of sulindac: Isolation and characterization of a new polymorph and three new solvates. J. Pharm. Sci. 86, 248-251.
Tulashie, S.K., Polenske, D., Seidel-Morgenstern, A., Lorenz, H., 2016. Solid-Phase and Oscillating Solution Crystallization Behavior of (+)- and (-)-N-Methylephedrine. J. Pharm. Sci. 105, 3359-3365.
Ubbelohde, A.R., 1965. Melting and Crystal Structure. Oxford University Press, London.
Uchida, T., Yonemochi, E., Oguchi, T., Terada, K., Yamamoto, K., Nakai, Y., 1993. Polymorphism of Tegafur - Physicochemical Properties of 4 Polymorphs. Chem Pharm Bull 41, 1632-1635.
Umeda, T., Matsuzawa, A., Ohnishi, N., Yokoyama, T., Kuroda, K., Kuroda, T., 1984. Studies on Drug Nonequivalence .12. Physicochemical Properties and Bioavailability of Benoxaprofen Polymorphs. Chem Pharm Bull 32, 1637-1640.
van Eupen, J.T.H., Westheim, R., Deij, M.A., Meekes, H., Bennema, P., Vlieg, E., 2009. The solubility behaviour and thermodynamic relations of the three forms of Venlafaxine free base. Int. J. Pharm. 368, 146-153.
Vega, D.R., Baggio, R.F., 1989. Malotilate - Structure and Phase-Transformation. Acta Crystallogr. C 45, 1612-1616.
Vladiskovic, C., Masciocchi, N., Cervellino, A., 2012. A structural powder diffraction study of two polymorphic forms of nortriptyline hydrochloride. J. Pharm. Sci. 101, 4481-4489.
Vrecer, F., Vrbinc, M., Meden, A., 2003. Characterization of piroxicam crystal modifications. Int. J. Pharm. 256, 3-15.
Yang, C.Q., Ren, T.K., Wang, J., Wang, Y.L., Tao, X.L., 2013. Thermodynamic stability analysis of m-nisoldipine polymorphs. J. Chem. Thermodyn. 58, 300-306.
Yang, C.Q., Zhang, Z.W., Zeng, Y.L., Wang, J., Wang, Y.L., Ma, B.Q., 2012. Structures and characterization of m-nisoldipine polymorphs. CrystEngComm 14, 2589-2594.
Zanolla, D., Perissutti, B., Passerini, N., Chierotti, M.R., Hasa, D., Voinovich, D., Gigli, L., Demitri, N., Geremia, S., Keiser, J., Cerreia Vioglio, P., Albertini, B., 2018. A new soluble and bioactive polymorph of praziquantel. Eur. J. Pharm. Biopharm. 127, 19-28.
Zhang, J., Wang, Y.L., Wang, G., Hao, H.X., Wang, H.H., Luan, Q.H., Jiang, C., 2014. Determination and correlation of solubility of spironolactone form II in pure solvents and binary solvent mixtures. J. Chem. Thermodyn. 79, 61-68.
Zhang, W.P., Chen, D.Y., 2017. Crystal structures and physicochemical properties of amisulpride polymorphs. J. Pharm. Biomed. Anal. 140, 252-257.
Zhu, B., Wang, J.R., Ren, G.B., Mei, X.F., 2016. Polymorphs and Hydrates of Apatinib Mesylate: Insight into the Crystal Structures, Properties, and Phase Transformations. Cryst. Growth Des. 16, 6537-6546.